# Seismic Design of Low-Rise RC Wall-Frame Buildings for Preferred Performance

Thesis submitted in partial fulfilment of
the requirements for the degree of

*Master of Science in* ***Civil Engineering*** *by Research*

by

Arpan Singh
2020710001
arpan.singh@research.iiit.ac.in

International Institute of Information Technology, Hyderabad
(Deemed to be University)
Hyderabad - 500 032, INDIA

July 2023

# Seismic Design of Low-Rise RC Wall-Frame Buildings for Preferred Performance

Thesis submitted in partial fulfilment of
the requirements for the degree of

*Master of Science in* ***Civil Engineering*** *by Research*

by


Arpan Singh
2020710001
arpan.singh@research.iiit.ac.in



International Institute of Information Technology, Hyderabad
(Deemed to be University)
Hyderabad - 500 032, INDIA


July 2023

Copyright © Arpan Singh, 2023.
All Rights Reserved

# Certificate

This is to certify that the thesis entitled "*Seismic Design of Low-Rise RC Wall-Frame Buildings for Preferred Performance*" submitted by *Arpan Singh (*Roll No. 2020710001) to the International Institute of Information Technology Hyderabad, for the award of the degree of Master of Science in Civil Engineering by Research is a bonafide record of the research work done by him under my supervision. The contents of this report, in full or in parts, have not been submitted to any other Institute or University for the award of any degree or diploma.


Sunitha Palissery<br>
*Assistant Professor*<br>
Earthquake Engineering Research Centre<br>
International Institute of Information Technology Hyderabad

# Abstract

Hospital buildings are expected to remain *Occupiable* after earthquakes to cater to the post-disaster response and rescue efforts. This requires a stiffer and stronger structural system compared to the commonly adopted moment frames in normal buildings; wall-frame systems are recommended in these buildings. But, in addition to merely providing the wall-frame structural system, it is also essential to adequately design the wall-frames to meet the desirable *Occupiable* seismic performance. Appropriate seismic structural configuration, Structural Plan Density (SPD) of structural walls, and seismic design parameters are presented of typical hospital building located in Seismic Zone IV, that helped meet the preferred performance. A displacement-based limit state of structural damage in line with classic displacement demand estimation is proposed, to confirm the performance.

Fiber inelasticity in walls and moment frames in study frames and buildings are defined, for performing displacement controlled nonlinear static pushover analyses and nonlinear time history analyses in commercial software PERFORM3D. Alongside, *limit states of structural damages*, namely *yielding* of longitudinal reinforcement in *beams or columns* in tension, *yielding* of vertical longitudinal reinforcement in *structural walls* in tension, *crushing* of confined concrete in compression in *beams*, *crushing* of confined concrete in compression in *columns*, and spalling of unconfined concrete in compression in *structural walls* are also monitored to grade the damages, and in turn the seismic performance of wall-frames. Results suggest, numerical models with fiber inelasticity help predict nonlinear behaviour reasonably well. Moment frames do not provide preferred seismic performance, but wall-frames with plan-aspect ratio more than 4 enhances lateral stiffness, strength, and ductility of wall-frames, thereby meeting the preferred performance. The major findings of the study are at least 3% SPD of structural walls is essential in typical wall-frame hospital buildings to ensure *Occupiability* performance after earthquakes. Furthermore, Column-to-Beam Strength Ratio of minimum 2 is also required in hospital buildings to remain *Occupiable*.

…

*Blank Page*

# Acknowledgements

I express my gratitude to my Thesis Supervisor, *Dr. Sunitha Palissery*, for her support and guidance throughout this work. She was always available to advise and discuss with me technical content required for the work. Her willingness to provide necessary resources and materials whenever needed is highly appreciated.

I am also grateful to *Professors Venkateshwarlu M, Pradeep Kumar Ramancharla*, *and P. Pravin Kumar Venkat Rao* of EERC, for enriching my technical learning through the courses they taught. Their encouragement and motivation has helped me during the progress of the thesis work.

I extend my sincere thanks to *Bharat Prakke*, *S. Saranya* and *Dharmil Baldev* for their constructive technical feedbacks. I cherish the lighter moments I had with them that helped me for the smooth thesis work ride! I am thankful to my research centre colleagues *Velani Pulkit D.*, *Raghu Nandan Vyas Pammi*, *Lakshmi Supriya Yerramsetty*, *Niharika Talyan* and *Aniket Bhalkikar* for their support. Also, I am thankful to *Arjun Khanal*, *Naresh*, and *Anand* for making EERC laboratory facilities comfortable.

My sister Arpita supported me throughout. I sincerely owe my parents for what I have and learned. Their blessings saw me through the toughest times of this work; I dedicate this thesis to my loving parents *Dr. Surjeet Singh* and *Smt. Sabita Patel.*

Finally, I am thankful to Almighty, who has bestowed me with countless blessings, that helped me complete this thesis.

*Arpan Singh*

Blank Page

# Table of Contents

# List of Tables

Blank Page

# List of Figures

| Figure | Title | Page |
|---|---|---|

# List of Symbols

| *Symbol* | *Description* |
|---|---|
| $b$ | Breadth of section |
| $b_f$ | Breadth of boundary element of structural wall |
| $d$ | Effective depth of RC section |
| $d_w$ | Depth of web of structural wall |
| $d'$ | Effective cover to centre of extreme layer of reinforcement steel in tension |
| $d''$ | Effective cover to centre of reinforcement steel in compression |
| $d'''$ | Clear cover to transverse steel from highly compressed edge of RC section |
| $f_c$ | Compressive strength of unconfined concrete |
| $f'_{cc}$ | Compressive strength of confined concrete at peak strength |
| $f'_{co}$ | Compressive strength of unconfined concrete |
| $f_{ck}$ | Characteristic compressive cube strength of unconfined concrete |
| $f_l'$ | Effective lateral confining stress |
| $f_s$ | Stress in reinforcement steel |
| $f_y$ | Yield strength of reinforcement steel |
| $f_{yt}$ | Yield strength of transverse reinforcement steel bar |
| $l_p$ | Effective length of plastic hinge |
| $x_u$ | Neutral axis depth |
| $t_f$ | Thickness of boundary element of structural wall |
| $t_w$ | Thickness of web of structural wall |
| $A_h$ | Seismic coefficient |
| $A_{sc}$ | Area of reinforcement steel in compression |
| $A_{st}$ | Area of reinforcement steel in tension |
| $D$ | Overall depth of beam |
| $E_c$ | Modulus of elasticity of concrete |
| $E_{c,sec}$ | Secant modulus of confine concrete at peak stress |
| $E_s$ | Modulus of elasticity of reinforcement steel |
| $H$ | Lateral force |
| $H_d$ | Design lateral force |
| $H_e$ | Elastic maximum lateral force |
| $H_{max}$ | Maximum lateral force |
| $I$ | Importance Factor |
| $K_i$ | Initial lateral stiffness of building |

| ***Symbol*** | ***Description*** |
|---|---|
| $L$ | Span of beam |
| $P$ | Axial force |
| $R$ | Response reduction factor |
| $S_a$ | Spectral acceleration |
| $S_a/g$ | Design acceleration spectrum value |
| $T$ | Fundamental natural period of structure |
| $W$ | Seismic weight of the building |
| $Z$ | Zone factor |
| $\beta$ | Column-to-beam strength ratio θ |
| $\delta_{max}$ | Maximum drift capacity in structures |
| $\delta_u$ | Ultimate drift |
| $\delta_{y,idealised}$ | Idealised drift |
| $\delta_y$ | Yield drift |
| $\varepsilon_c$ | Strain in concrete |
| $\varepsilon_{cc}$ | Strain in extreme fiber of core concrete |
| $\varepsilon_{c,max}$ | Maximum compressive strain in extreme compression fiber of concrete |
| $\varepsilon_{ccu}$ | Maximum compressive strain in confined concrete |
| $\varepsilon_{csc}$ | Strain in concrete in compression at centre of reinforcement steel in compression |
| $\varepsilon_{cu}$ | Strain at spalling of unconfined concrete |
| $\varepsilon_{sc}$ | Strain at center of reinforcement steel bars in compression |
| $\varepsilon_{s,max}$ | Maximum strain in reinforcement steel |
| $\varepsilon_{st}$ | Strain at center of extreme layer of reinforcement steel in tension |
| $\varepsilon_{su}$ | Fracture strain of transverse reinforcement steel bar |
| $\varepsilon_o$ | Strain in unconditional concrete at extreme compression fiber at peak stress level |
| $\theta$ | Rotation in structural member |
| $\rho_s$ | Ratio of transverse confining steel to colume of confined concrete |
| $\Delta$ | Lateral deformation |
| $\Omega$ | Overstrength |

…

# 1

# Introduction

## 1.0 OVERVIEW

Important buildings like governance buildings, hospitals, and fire stations are expected to remain Occupiable and Operational after earthquakes. But, past earthquakes have witnessed full or partial collapses of these buildings, thereby jeopardizing their functionality. Even in the recent 2010 Haiti earthquake that killed more than 2 lakh people, [Cred, 2020] hospital buildings also collapsed that compounded the number of fatalities (Figure 1.1). Similar behaviour of hospital buildings is reported in other past earthquakes also. Of the available design guidelines, National Disaster Management Authority (NDMA) recommends wall-frame structural systems to be adopted in hospital buildings with minimum Structural Plan Density (SPD) of 4%, and Column-to-Beam Strength Ratio to be 2.5. In addition, seismic design codes recommend use of Importance Factor of 1.5 in design of these important buildings. But, critical structural parameters that ensure structural safety of hospital buildings enabling their intended functionality is still unclear.

**Figure 1.1**: Collapse of Turgeau hospital during 2010 Haiti Earthquake [Photo: Desroches, *et al.*, 2011]

Further, there is no guarantee that the adoption of available design guidelines and design values will provide an *Occupiable* hospital building after a strong earthquake. Presence of wall-frame structural system will increase stiffness and strength of building thereby providing superior performance during an earthquake, but placing and orientation of structural walls in structural plan plays an important role in seismic performance of buildings [Fintel,1995]. Hence, providing a good structural configuration is also important to achieve the preferred performance and so is the need to numerically investigate this structural aspect. Therefore, there is an urgent need to evaluate seismic performance of typical hospital buildings to provide pointers for adequate design that help achieve their preferred seismic performance. This study is an attempt towards improving seismic safety and achieving the preferred performance of hospital buildings.

The following section presents the common earthquake resistant virtues of buildings, if provided adequately help achieve the required performance in all buildings.

## 1.1 EARTHQUAKE RESISTANT VIRTUES OF BUILDINGS

During seismic events, a building with good *structural configuration* and designed complying with the principles of earthquake resistant design that ensures adequate *lateral stiffness*, *strength*, and *ductility*, will behave forming a desirable *collapse mechanism*. These are considered the important earthquake resistant virtues.

### (a) Structural Configuration

Structural configuration of a building provides the ability to transfer the inertia forces safely to foundation, by forming continuous load paths. Geometry, size, shape, and location of structural and non-structural elements define the configuration of a building. In buildings with *simple* rectangular floor plans and straight elevations, inertia forces are transferred through straight load paths to the ground. But, buildings with complex geometry unlike the above, inertia forces are transferred forming curved load paths before reaching the ground. Therefore, in general, simple and regular building geometry is preferred for good seismic resistance. Further, symmetric mass or stiffness distribution in structural plan precludes undesirable torsional modes of oscillation and stress demands on structural elements, during earthquakes. Torsional irregularity, re-entrant corners, excessive slab cut-outs, out-of-plane offsets in vertical elements, non-parallel lateral force systems, are irregularities in buildings that are detrimental to their seismic performance.

**(b) Lateral Stiffness**

Lateral stiffness of a building provides the robustness required to resist the lateral loads without any lateral instability. The initial lateral stiffness can be pictorially represented by the initial slope of the monotonic lateral load-lateral deformation curve (Figure 1.2). Further, a minimum lateral stiffness in buildings protects the non-structural elements reasonably well, but, the above stiffness reduces as the structure incurs more damage, during earthquake. In general, lateral stiffness of a structure is influenced by properties of the materials, cross-section, structural member, connections, and the structural system. It is recommended to construct buildings with uniform distribution of stiffness in two orthogonal plan directions to ensure the comfort of occupants and prevent damage to the contents of the building during its elastic excursions, and reasonable seismic safety during inelastic excursions, under earthquake shaking [Murty, *et al*., 2012; Elnashai and Di Sarno, 2008].

**(c) Lateral Strength**

Lateral strength is the maximum resistance that a building can offer during the entire lateral loading history. The maximum lateral strength is pictorially determined by the maximum strength obtained from lateral load-lateral deformation curve (Figure 1.2). Further, a minimum lateral strength in each of its plan directions is required to resist low intensity ground shaking without incurring significant structural damages. Furthermore, the building must possess a minimum vertical strength also to support the gravity load and prevent collapse during strong earthquake shaking. But, the strength must not be excessive to economical construction.

**(d) Lateral Ductility**

Earthquakes impose displacement loading on the building base, and hence the building must possess adequate displacement capacity. Seismic force and displacement demands must be addressed together in design for obtaining reasonably good seismic behaviour. Lateral ductility of a structure is the ratio of the maximum deformation and the idealized yield deformation pictorially obtained from lateral load-lateral deformation curve (Figure 1.2). Overall ductility of the structure is achieved only when sufficient material ductility, curvature ductility and rotational ductility are ensured during the design.

### (e) Desirable collapse mechanism

Collapse mechanism is defined as the failure mechanism formed during the earthquake time history when the structure passes through the inelastic excursions of structural damages. Based on the structural system and design detailing provided in the building, this collapse mechanism will vary and there exists a *desirable* collapse mechanism in different types of buildings and structural systems (Figure 1.2). For, example, desirable collapse mechanism in a moment frame building is the one when ends of beams and only in column bases in fixed base buildings accrue inelastic damages across the height of the buildings, thereby forming a failure mechanism. Similarly, different structural systems form different failure mechanisms depending on the design performed. The desirable behaviour is decided by the intended performance of the building; normal buildings may have the above collapse mechanism as acceptable, but the same behaviour becomes unacceptable in hospital buildings.

Thus, quantification of the earthquake resistant virtues is primarily decided by the required performance of the building. Hospital buildings are required to remain Occupiable after earthquakes and hence the need to quantify the requirements more critically.

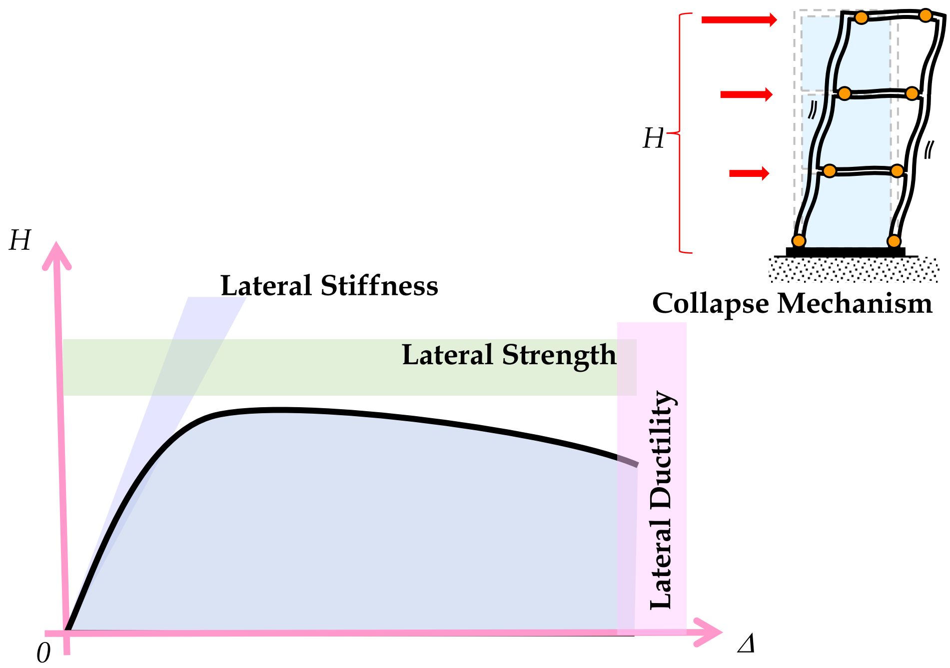


**Figure 1.2**: Virtues of Earthquake Resistant Structures [Elnashai and Di Sarno, 2008]

## 1.2 ORGANISATION OF THESIS

This thesis is presented in 5 independent chapters. In Chapter 1, an introduction is presented to provide an overview of the work required to meet the contention of thesis. In Chapter 2, a brief review of pertaining literature is presented, gap areas of the study identified, and objectives and scope of the present study outlined.

In Chapter 3, effects of structural wall plan aspect ratio, structural configuration, and location of structural walls in wall-frame systems required for good seismic behavior are outlined, from results of pilot study. Further, Chapter 4 discusses the proposed methodology to achieve preferred seismic performance in hospital buildings and numerical investigations carried out are presented.

Finally, summary and conclusions are presented in Chapter 5. Limitations of the present work are listed and scope of future work in the subject area is also discussed.

...

# 2

# Review of Literature

## 2.0 OVERVIEW

Hospitals, fire stations, police stations, and similar facilities are constructed using reinforced concrete due to its versatility and easy availability. On one hand, these buildings are critical due to the requirement of *Occupiability* after an earthquake disaster, their lack of seismic safety is obvious from past earthquake experiences. Currently, moment frames are the most widely adopted structural system in these buildings, even in high seismic regions. High deformation demands imposed on moment frames during severe earthquake shaking leads to partial or complete collapses of the buildings. Of the above buildings, hospitals need special care in their design and their subsequent seismic performance, due to the functionality it serves and the critical building contents it accommodates. This thesis investigates hospital building design and its seismic performance.

Across the globe, approximately 48% of hospital buildings are at high risk due to the collapse of structural members, while 91% non-structural elements in lifeline structures can be seriously damaged, resulting in life-threat to users [Krishnamurthi, *et al.*, 2018]. Structural deficiencies noticed in buildings that performed poorly during past earthquakes in India and worldwide pertain to inadequacies in two key aspects, namely (1) structural system; *e.g.*, reinforced-concrete (RC) moment frame buildings and RC buildings with flat slabs, and (2) structural design; *e.g.*, open ground storey buildings, and non-ductile beams and columns. While such damages and collapses of normal buildings have been widespread during past earthquakes, seismic safety of hospital buildings which are expected to remain functional after an earthquake, are also in jeopardy. In particular, learning experience from collapse of hospital buildings and damages incurred in these buildings during 1971 San Fernando, 1994 Northridge, 2001 Bhuj, and 2011 Canterbury earthquakes, raised concerns on the seismic safety of hospital buildings. Thus, improving safety of hospital buildings against earthquakes is a crucial technical need. Therefore, it is attempted to understand seismic behaviour of commonly adopted RC structural systems, their earthquake performances, damage pattern observed, causes of failures etc as part of work carried out for this thesis. In addition, numerical modeling capable of capturing nonlinear behavior of structures needs appropriate modeling techniques to be adopted to define inelasticity in select structural members. Further, understanding inelastic behaviour begins with material modeling or adopting suitable constitutive relations in numerical modeling. Also, structural analysis methods used for performance assessment of designed buildings need to be examined. This Chapter discusses relevant literature pertaining to all of above, with focus on hospital buildings.

## 2.1 STRUCTURAL SYSTEMS

Structural systems safely sustain, and transfer applied loads to the ground through the unique assembled and constructed structural members in a structure. For earthquake resistant concrete buildings, structural systems can be classified into 3 categories: (a) frames, (b) coupled or isolated structural walls, and (c) frames interacting with structural walls [Fintel *et al*., 1977]. Frames built to resist lateral force actions are generally called *moment resisting frames*. Structural systems and their seismic behaviour are discussed hereunder.

### (a) Moment Resisting Frame Systems

A Moment Resisting Frame (MRF) consists of beams and columns that are rigidly connected to each other (Figure 2.1). In MRFs, columns are lateral load resisting elements and resistance to lateral forces depends on the rigidity of the connections. Common mid-rise structures subjected to moderate levels of earthquake shaking adopt MRFs as structural systems [Fintel *et al*., 1977].

### (b) Coupled Structural Wall Systems

A coupled wall system is made up of two or more structural walls that are connected in parallel by coupling beams (Figure 2.2 (a)). In this structural system, structural walls alone are lateral load-resisting elements. These structural walls have high lateral stiffness and strength. Coupling beam design is critical as they must transfer high stresses between neighboring walls during earthquake loading. Tall buildings with more than 60 typical storeys adopt coupled structural wall structural systems. [Fintel *et al*., 1977; El-Tawil,2010].

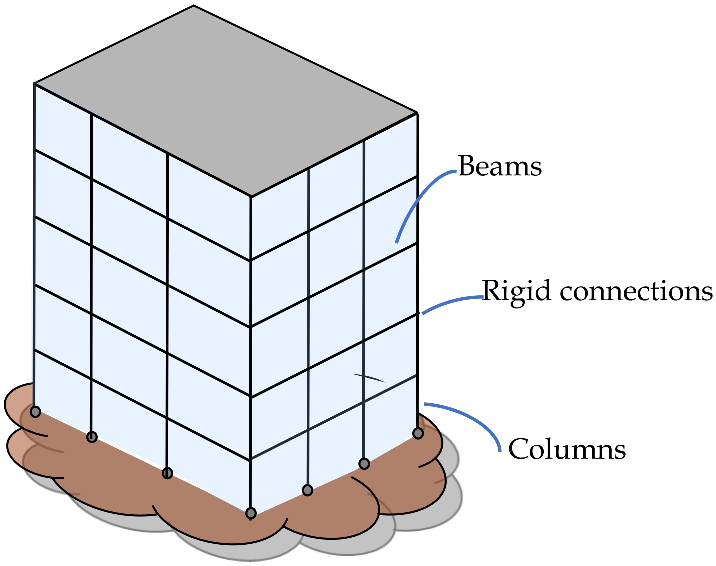


**Figure 2.1**: Moment resisting frame building

### (c) Frames interacting with Structural Wall Systems

Frames interacting with structural wall systems consists of MRFs and structural walls (Figure 2.2(b)). In this structural system, MRFs and structural walls which are detailed as per ductile detailing recommendations, together resist lateral loads. This system has high lateral stiffness and strength provided by structural walls, which reduces the imposed lateral displacement demands. But, due to high stiffness and strength, lateral force demands imposed on structural walls are significantly high, though the proportion of forces resisted by frames and structural walls is dependent on their individual stiffness. In general, MRFs in these structural systems are designed to resist at least 25% of the total base shear acting on the building [Fintel *et al.*, 1977; V. V. Bertero, 1980].

## 2.2 PAST EARTHQUAKE PERFORMANCE

Performance of structures during past earthquakes help designers to understand the lacunae in design procedures and provisions in design codes. In the past, every major earthquake has led to the evolution of earthquake engineering in this direction. In this section, review of literature pertaining to the past earthquake performance of structural systems, and in particular, hospital buildings are discussed.

### 2.2.1 Structural Systems

In the early decades of nineteenth century, structures were designed to resist gravity loads. Experience after 1906 San Francisco earthquake, 1908 Messina earthquake, and 1923 Kanto earthquake in Japan gave impetus to examine the existing design provisions and thus significant improvements came to practice in 1960s worldwide [Reitherman, 2006]. Aftermath of the 1960 Chile earthquake where failure of moment frame and masonry structures were widespread led to the implementation of a more rigid and strong *wall-frame dual system*. Even during 1994 Northridge earthquake, moment frame buildings incurred severe structural damages. Significant diagonal tension cracks at third-story columns indicated insufficient shear and confining reinforcement in the columns. It is reported that the significant drift demands imposed in these buildings were mainly due to the absence of structural walls [Mitchell, *et al.*, 1995]. Seismic performance of RC buildings can be enhanced if structural walls are incorporated and appropriately designed according to modern seismic codes [Otani, 1977; Ozkul, *et al*., 2019]. Similarly, excessive deformations resulted in collapse of a parking moment frame structure during 1994 Northridge earthquake [Figure 2.3]. Later, in the 2010 and 2015 Chile earthquake, wall-frame structures exhibited exceptional resistance to lateral loads without collapse [Naeim, *et al.*, 2010; Lagos, *et al.*, 2017; Ugalde, *et al.*,2017]. Good seismic resistance of wall-frame systems was demonstrated experimentally also [Y Lu, 2001].

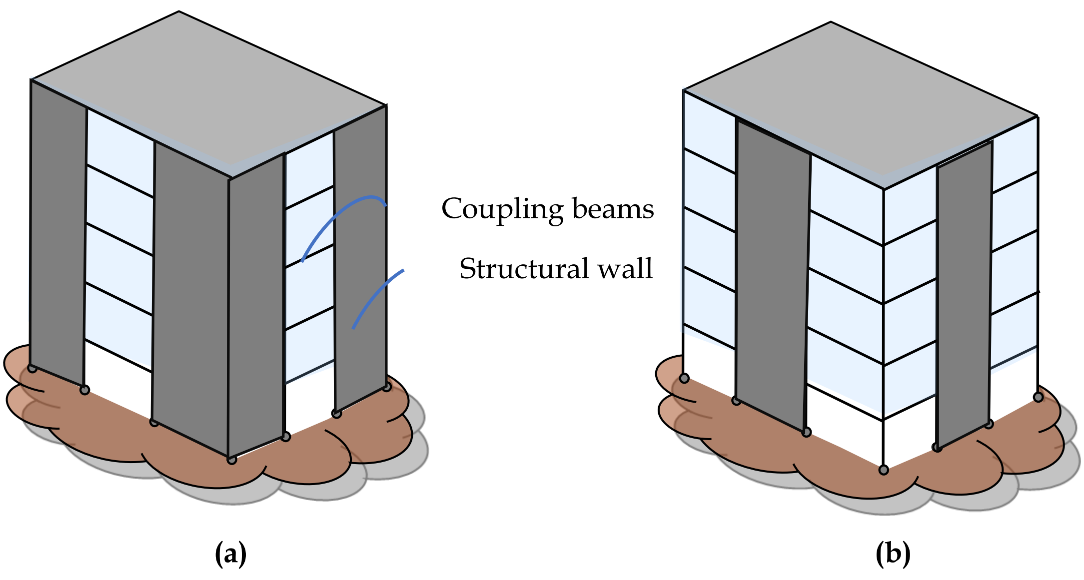


**Figure 2.2**: Structural systems: (a) Coupled structural wall system; and (b) Frame system interacting with structural walls

**Figure 2.3**: Earthquake performance of RC buildings during the 1994 Northridge earthquake: parking building collapse due to lack of redundancy and excessive deformation in one direction [Photo: EERI Annotated Slide Collection, 1998]

"We cannot afford to build economical concrete structures to resist severe earthquakes without shear wall," is one of the early testimonials to the convincingly superior performance of wall-frame systems [Fintel,1995]. Similar stiff and strong structures are needed for critical buildings like hospitals. The following section presents past earthquake behaviour of hospital buildings, worldwide.

### 2.2.2 Hospital Buildings

Structural systems in existing hospital buildings are MRFs with reinforced or unreinforced masonry, and in exceptional cases are either base-isolated or wall-frame systems. Reports of collapses and severe damages of hospital buildings affecting their *Occupiability* are available. Most of the hospital buildings collapsed during 1971 San Fernando earthquake due to inadequate design. Underestimation of seismic forces at the site of the Veteran Administration Hospital is an example (Figure 2.4 (a) & (b)) that led to the death of 46 patients. Olive Medical centre, constructed before 1960 as per old code, could not resist the imposed seismic forces [Lew, *et al.*, 1975]. Later, the 1985 Michoacan, Mexico City earthquake severely damaged and collapsed the city's largest hospital structure. Owing to the collapse of a portion of Mexico general hospital, 1200 people were buried beneath the wreckage (Figure 2.5 (a)). The cause of such devastating failure is reported to be attributed to a variation in stiffness in two principal plan directions which led to rotation of structure by about 25 degrees. Core incurred pancake collapse, beams and girders no visible damages, and columns significant damages. Lack of strong column-weak beam criteria was prominent in the design of the structure [Stone, *et al*., 1987]. Similar failure due to strong beams and weak columns were observed during 1971 San Fernando earthquake and 2003 Bam earthquake. Holy cross hospital, a seven-storey building comprising a boiler plant and one storey continuity care facility, incurred severe damages to the exterior columns of the structure. The building did not remain operational post-earthquake, and around 170 patients were evacuated [Lew, *et al*., 1975]. Also, due to the failure of the beam-column joint on each floor in Juarez hospital, 400 infants were trapped inside the hospital. But, the lack of minimal to non-existent confinement through the joint was the primary reason for the structure's collapse [Stone, *et al*., 1987].

Like 1985 Mexico City earthquake, the 1995 Kobe earthquake also caused substantial damage to mid-rise RC buildings due to irregularity in plan and stiffness (Figure 2.5 (b)). Miyagi hospital had structural walls on the ground floor alone, making it stiffer than other floors. Also, the floor plan size immediately reduced in second floor thus making it more rigid than the floor above it, but not strong as the ground floor, leading to failure. Similar damage was observed in West Kobe Citizen's hospital which completely collapsed at the fifth floor while the other storeys remained relatively undamaged [Chung, *et al.,* 1996]. Further, damages due to failure of structural elements during 1994 Northridge earthquake led to shutdown of St. John's and the Berkley East Convalescent Hospitals [Todd, *et al*., 1994].

**(a)** **(b)**

**Figure 2.4**: Building collapse due to underestimation of forces or improper seismic design practices during 1971 San Fernando earthquake: (a) Veteran Administration Hospital [Photo: Lew, *et al*., 1975]; (b) St. John's hospital window piers-transverse reinforcement spaced at 150-200 mm with $90^0$ hooks [Photo: Todd, *et al*., 1994]


**(a)** **(b)**

**Figure 2.5**: Building collapse due to irregularity in plan or stiffness: (a) General Hospital pan cake collapse during 1985 Mexico City earthquake [Photo: Fintel, 1995]; and (b) Upper storey collapse of West Kobe Citizen's Hospital during 1995 Kobe earthquake [Photo: Chung, *et al*., 1996]


**(a)** (b)

**Figure 2.6**: Building collapse due to failure of columns: (a) Severe damages in exterior columns of Holy cross hospital in 1971 San Fernando earthquake [Photo: Fintel, 1995]; and (b) Failure of beam-column joint of Juarez hospital in 1985 Mexico City Earthquake [Photo: Photo: Stone, *et al*., 1987]

Furthermore, after the 2001 Bhuj earthquake, no hospitals were functional in Bhuj region [Roy, *et al*., 2003]. Past performance of hospital buildings is affected due to change in location and stiffness offered by lateral load resisting elements.

Failure of masonry infills led to the collapse of hospital buildings making them unoccupiable after the 2003 Bam earthquake [Eshghi, *et al*., 2005]. The 1969 RC structure, Berkley East Convalescent Hospital incurred damages in exterior masonry walls [Todd, *et al*., 1994; Eshghi, 2005]. Hospital buildings with structural walls also incurred severe damages during 1971 San Fernando earthquake.

**Figure 2.7**: Building collapse: (a) Partial collapse of Sidhu Sadabahar hospital during 2015 Gorkha Nepal earthquake [Photo: Chen, *et al*., 2017]; (b) Collapse of Iskenderun state hospital [Photo: Reuters, 2023]

Cracking and spalling of concrete at location of splicing were widespread [Lew, *et al*., 1975]. Further, pounding resulted in partial collapses of hospital buildings during 2015 Gorkha Nepal earthquake (Figure 2.7) [Chen, *et al*., 2017].

Thus, past earthquake experience on seismic performance of hospital buildings provides imperative to investigate seismic behaviour of hospital buildings under severe earthquake shaking and help complement the current design provisions, alongside quantitative estimation procedure of performance. Design parameters required to meet the *Occupiable* performance criteria need clarity for ease of implementation in design practice.

## 2.3 CURRENT DESIGN RECOMMENDATIONS FOR HOSPITAL BUILDINGS

Usually, Seismic Design Codes worldwide have been considering the criticality in design of critical hospital buildings, by using Importance Factor $I$, in the estimation of design lateral force using equivalent static analysis method as:

$$H_d = A_h W = \left[\frac{ZI}{2R}\left(\frac{S_a}{g}\right)\right] W, \tag{2.1}$$

Where $A_h$ is the seismic coefficient, W seismic weight of the structure, $I$ is the *Importance factor* (for normal buildings taken as 1.0, and 1.5 for critical structures such as hospitals), $Z$ the *Seismic Zone Factor*, $R$ the *Response Reduction Factor* (taken 5 for SMRF and Dual system) and $S_a/g$ the design acceleration spectrum value (depends upon fundamental translational period of the structure). In addition, for irregular buildings most design codes recommend linear dynamic analysis, namely response spectrum analysis and time history analysis to estimate the seismic demands. The discussion hereunder on linear static analysis parameters assuming that hospital buildings are in general built as regular structures [IS 1893(1):2016].

Using *I* greater than 1.0 in design reduces inelastic behaviour, which in turn reduces the damage potential of buildings. Further, National Disaster Management Authority (NDMA) Guidelines of India on seismic design principles for design of hospital buildings requires that Critical Units of Hospital Buildings be designed for higher specifications than those for which the Other Units of Hospital Buildings are required to be designed. In particular, the guidelines recommend the following in design of hospital buildings: (a) wall-frame structural system, (b) estimation procedure of seismic lateral force demand, and (c) relative column-to-beam strength ratio in moment frames [NDMA,2016].

Seismic design of hospital buildings requires special attention; it is desirable to have the following performance levels satisfied under the severe earthquake shaking:

(a) Building system should be immediately Occupiable; and

(b) Non-structural and medical utilities should remain Operational without any shut down.

The Occupiability of structural system will help immediate use of hospital building without any perceived threat to the users and its contents, even during a post-earthquake event. And, the Operationality of the non-structural and medical utilities will help in continuity of healthcare facilities. The performance requirement mandated in the NDMA guideline expects Occupiability of hospital building structures and Operability of non-structural elements within hospital buildings, post-disaster; it needs to be verified that in buildings with wall-frame structural system, the expected performance is met. Also, the expected behaviour of hospital buildings to achieve Occupiability, is still not guaranteed only by the use of *I* factor in structural design. The recent shift in expected behaviour of critical hospital buildings from *no collapse* to achieving *Occupiability* is still not guaranteed only by the use of *I* factor in structural design. Further, design codes also impose a limit on elastic drift for all buildings, to ensure at least a reasonable lateral stiffness (*e.g.*, 0.4% is the elastic drift limit stipulated in IS 1893 (1): 2016). Thus, currently, most seismic design codes focuses on *stiffness* and *strength* requirement expected of hospital buildings qualitatively by: (1) limiting the elastic drift, and (2) designing for a higher seismic force. But, it is unclear, whether a building thus designed meets both stiffness and strength requirements for the building to remain Occupiable after the earthquake. Further, recommendation for a suitable structural system to meet the preferred performance is not mandated by design codes. Deformation demand imposed in these buildings is also unclear. Because, the performance expectation of normal buildings are to achieve *no collapse* and hence expected to incur *significant* inelastic deformations under severe earthquake shaking, whereas with the same structural system, hospital buildings are to 'remain functional' and hence expected to incur *insignificant* inelastic deformations.

This work intends to develop a physically intuitive, yet quantitative, seismic design parameters and performance assessment methodology, especially for design of hospital buildings for easy implementation by the designers. This is proposed to be addressed first by confirming adequacy of existing guidelines, and further by quantifying critical design parameters required to ensure intended performance of hospital buildings.

## 2.4 INELASTIC STRUCTRUAL ANALYSIS for SEISMIC SAFETY ASSESSMENT

For seismic design of buildings, estimation of proper demands imposed on structural members can be determined using linear elastic structural analysis. But, design adequacy of structural members is verified using assessment of inelastic behaviour. The following *nonlinear static* and *nonlinear dynamic* analysis methods are commonly carried out for the purpose. The most typical approach for evaluating the seismic behaviour of buildings is through dynamic analysis, but it requires significantly more computational effort than static analysis. However, static analysis takes less time but is generally applicable for regular structures [Elnashai and Di Sarno, 2008].

### (1) Nonlinear Static Analysis or Pushover Analysis

*Nonlinear Static Analysis* (NSA) or *Pushover analysis* is carried out by application of horizontal forces or displacements with a constant profile along the height of a building, until the building collapse. The sequence and possible location of damage in a structure (at pre-defined locations) can be obtained using load-deformation or nonlinear static response curves (Figure 2.8).

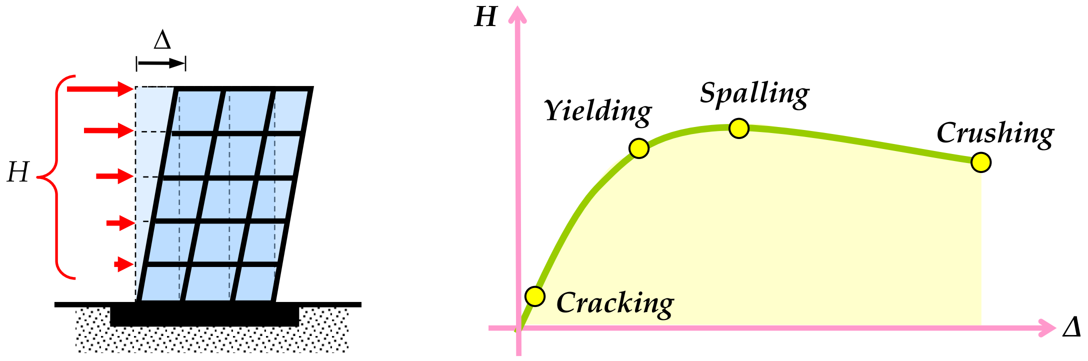


**Figure 2.8**: Nonlinear static response analysis curve and salient damages monitored [Sunitha, P., 2017]

In a RC building, cracking of concrete, yielding of reinforcement, spalling of cover concrete, crushing of confined concrete are usually monitored. Further, nonlinear static response curves are obtained either from conventional pushover analysis or adaptive pushover analysis. In conventional displacement-controlled pushover analysis, a constant *pattern* of horizontal loads under incremental displacements is applied to the building. But, adaptive pushover analysis method considers variations in the mode shapes of building during the inelastic behaviour. In general, pushover analysis is performed of those structures in which higher-mode effects are not significant [FEMA 356,2000]; buildings with first mode translational and more than 80% mass participation are suitable candidates for pushover analysis.

**(2) Nonlinear Dynamic Analysis**

In general, *nonlinear time history analysis* (NTHA) and *incremental dynamic analysis* (IDA) are the commonly adopted nonlinear dynamic analysis methods. In both the methods, structure is subjected to natural or synthetic ground motions scaled using any of the available methods, and inelastic behaviour monitored. Damages at pre-defined inelastic locations are investigated and seismic performance evaluated.

***(a) Nonlinear Time History Analysis (NTHA)***

In this analysis method, the force or displacement response histories of structure are evaluated under natural or synthetic ground motions in time domain. Materia l(and geometric nonlinearities) are considered based on the instantaneous state of deformation of the building. Design standards and documents recommend number of ground motions to be used to assess the inelastic behaviour of structure. For *e.g.,* ASCE 07 recommends 11 ground motions for linear analysis and the same is usually used by designers for NTHA [ASCE 7,2022]. FEMA 356 on the other hand recommends at least 7 ground motions for considering mean responses of structure [FEMA356, 2000]. NTHA can be performed of regular and irregular structures to obtain realistic estimates of seismic demands.

***(b) Incremental Dynamic Analysis***

Incremental Dynamic Analysis, or Dynamic Pushover Analysis, is an analysis technique that involves applying multiple ground motions to the structure, each of which is scaled to multiple intensities and responses investigated. Numerous such analyses are conducted, and the resulting responses are plotted with record intensity levels. The resulting curve, known as the IDA curves, indicates the seismic performance of structure at all excitation levels [Bertero, 1977; Nassar and Krawinkler, 1991; Vamvatsikos and Cornell, 2002].

In general, scaling of ground motion to assess the realistic seismic safety of a structure is crucial. This help check the maximum lateral demands that a designed structure can resist before collapse.

### 2.4.1 Scaling of ground motions for NTHA

In general, 3 methods are employed for scaling of ground motions to reliably capture the seismic behaviour of structures. They are: (a) PGA/PGV/PGD Scaling (b) spectral amplitude scaling, and (c) spectrum matching.

*PGA/PGV/PGD scaling* is based on peak ground parameters i.*e,* PGA, PGV or PGD. In this method, to select the suitable peak ground parameter to be scaled, 3 intervals of structural periods (short period structures sensitive to PGA, moderate period structures sensitive to PGV and long period structures sensitive to PGD) are identified. It is the simplest scaling method where the time history of ground parameter is linearly scaled to the required value and the structure is subjected to scaled time history record. Inelastic responses can then be investigated. Despite the several drawbacks reported by past researchers this scaling technique is still used by researchers [Elnashai and Di Sarno, 2008].

S*pectral amplitude scaling* is based on the spectral value at the elastic natural period of the structure. In this method, spectral value of the ground motion response spectrum at fundamental period of structure is scaled to match the corresponding design spectral value. The obtained scaling factor is then used to linearly scale the time history record of ground motion and structure is subjected to it. Inelastic responses can then be investigated. Here, only the amplitude of the ground motion is modified, but its duration, frequency content etc. remain unchanged. This method is suitable for buildings located in far-fault sites but needs more detailed analysis for near-fault sites [Hancock, et al., 2006; Kalkan and Chopra, 2010; Huang, et al., 2011].

*Spectrum Matching* is based on a multiplier that matches the system's spectral acceleration of system at a fundamental period to the desired spectral acceleration. The scaled spectral accelerations are equal to the target spectrum at the system's fundamental period. This reduces the number of records required to achieve satisfactory precision in performance estimation. This scaling method may modify the physical attributes of the accelerograms, and loses accuracy at higher vibrational frequencies because yielding and nonlinear behavior lengthen the vibration periods [Kurama and Farrow, 2003; Hancock, *et al*., 2006; Yeong Ae, *et al*., 2011]. This method is recommended for all far field and near-field sites for ground motions that do not include velocity pulses [Haselton, *et al*., 2012].

Finally, a designed structure needs to be verified of its seismic safety under realistic seismic forces by using one of the above nonlinear analysis methods. This requires defining inelasticity at select locations in select members; following section discusses the inelasticity in structural members.

## 2.5 INELASTICITY IN STRUCTURAL MEMBERS

For performing nonlinear analysis, inelastic regions in structural members needs to be defined. Inelastic regions can be defined using lumped plastic hinges or inelastic fiber segments, depending on type of modeling technique adopted. Location of flexural inelasticity is in general at ends of beams, columns and structural walls for lumped plastic hinges (sometimes at the middle of the structural wall also). Similarly, shear hinges can also be defined. Inelastic fiber segments are usually defined across the depth of cross section in beams and columns and in the entire structural wall [Rana, *et al.,* 2004]. Any type of inelasticity begins from material and a suitable stress-strain relationship of concrete and reinforcement needs to be selected to define unconfined concrete, confined concrete and overstrength reinforcement behaviour. Kent and Park model (1971), Mander model (1988), Saatciooglu & Razvi model (1992) are 3 of the many confinement models available for use. The choice of type of inelasticity also depends on the commercial software used for nonlinear behaviour assessment. The following section discusses the available options in commercial software PERFORM 3D which is used in this thesis work [CSI, 2018].

### 2.5.1 Inelasticity in Beams and Columns

In PERFORM 3D, four different model types are used to define beam and column inelasticity. They are: (a) chord rotation model, (b) plastic hinge model, (c) plastic zone model, and (d) finite element model [CSI, 2018].

#### (a) Chord Rotation Model

The chord rotation model is easiest to model inelasticity but has many limitations. This model is valid for *symmetrical* members with equal and opposite end moments acting on the structural member. The following fundamental components are used to implement the chord rotation model which are *pre-defined* in PERFORM 3D based on FEMA 356 (2000) recommendations: (a) FEMA concrete-type beam (insignificant axial force demand), and (b) FEMA concrete-type column (significant axial force demand and interacting axial-flexure behaviour). Each component consists of two parts: a plastic hinge and an elastic segment (Figure 2.9(a)) [CSI, 2018].

#### (b) Plastic Hinge Model

The plastic hinge model is applicable even to unsymmetrical members and is analogous to *user-defined* chord rotation models (Figure 2.9(a)). Here, user can define inelasticity using moment-curvature or moment rotation relationship of structural sections and has the advantage of designing and positioning hinges as per user need. For defining plastic hinges in structural elements, zero-length hinges are utilized [CSI, 2018].

#### (c) Plastic Zone Model

In plastic zone model, plastic zones at both ends are modeled using fiber section segments. The fundamental characteristic of a fiber segment depends upon the material stress-strain properties; plastic deformation is spread across a finite length of plastic zones in this model, while the remaining portion of the structural element is considered elastic.

(Figure 2.9(b)). Length of plastic segments can be estimated using one of the recommendations from past literature (Table 2.1) [CSI, 2018].

**(d) Finite Element Model**

In the finite element model, structural members are divided into number of inelastic sections and inelasticity defined using fiber segments or curvature hinges (Figure 2.9(c)). Moment-curvature and stress-strain relationships can be used to determine the curvature hinges and fiber segment properties, respectively. Choice of mesh size depends on analysis approach and must require mesh convergence study for accurate results [CSI, 2018].

It is required to define the plastic hinge length in the above inelastic models, to confirm a reasonable spread of inelasticity compared to point inelasticity. The available recommendations are discussed below.

#### *2.5.1.1 Plastic Hinge Length*

Plastic hinge zone, the inelastic zone with a high strain gradient, typically forms over a length known as plastic hinge length $l_p$ (Figure 2.10). The theoretical length of plastic hinge is based on the distribution of its curvature. Recommendations for $l_p$ from past literature are listed in Table 2.1. In this study, 0.5 $D$ is assumed as plastic hinge length [FEMA 356,2000].

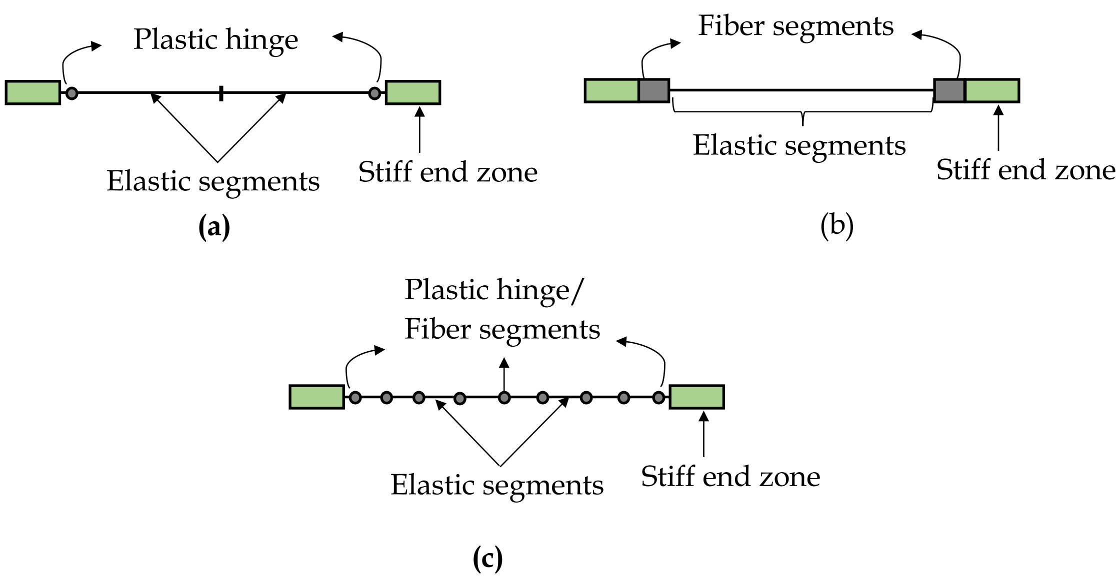


**Figure 2.9**: Inelasticity modelling techniques for beams & columns, (a) chord rotation model and plastic hinge model, (b) plastic zone model, and (c) finite element model

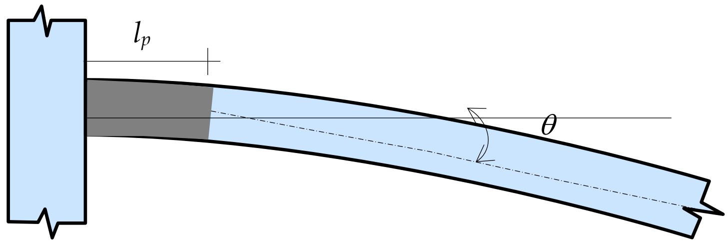


**Figure 2.10**: Plastic hinge length

| Source | Effective length of plastic hinge($l_p$) |
|---|---|
| **Sawyer, 1964** | $l_p$=0.25$d$+0.075$z$, where $d$ is the effective depth, and $z$ distance from critical section to point of contraflexure |
| **Mattock, 1967** | $l_p$=0.5$d$+0.05$z$, and $\varepsilon_{c,\ max}$=0.003+0.02($\frac{b}{c}$)+0.2$\rho_s$ where $d$ is effective depth of the section, $z$ is distance from critical section to point of contraflexure, $b$ width of beam, and $\rho_s$ ratio of volume of confining steel (including compression steel) |
| **Paulay and Priestley, 1992** | $l_p$= 0.08$l$+0.022$d_b f_y$ ($MPa$), where l is length of cantilever (distance to inflection point in a beam or column), $d_b$ reinforcing bar diameter, and $f_y$=steel yield stress |
| **Park and Paulay, 1975** | $l_p$= 0.5$D$ |
| **FEMA 356, 2000** | $l_p$= 0.5$D$, where $D$ is the overall depth of the structural member |

**Table 2.1**: Plastic hinge length recommendations

Further, similar to the inelastic models to define inelasticity in structural members, modelling structural members to predict seismic behaviour are also crucial. In particular, modelling of structural walls needs attention.

### 2.5.2 Common Modelling approaches of Structural walls

The commonly used structural wall modelling methods are: (a) single column model, (b) fiber model, (c) strut and tie model, and (d) shell model [Orakcal, 2004; Anwar *et al.*, 2006; Fajhan, *et al.*, 2012]. Each of the above are discussed here.

### (a) Single column model

In this model, structural walls are represented by wide columns along the centerline of wall, representing its stiffness. Interacting axial-flexural hinges (PMM) are used to define inelasticity. But, long, interacting, cellular core walls or walls with opening, and complex structural walls cannot be accurately represented by this model [Fahjan, *et al.*, 2010; Anwar, *et al.*, 2009].

**(b) Fibre Model**

In this model, fiber segments are used to define concrete and reinforcing layers of structural walls. Walls with openings and cellular core walls can be accurately represented by this model. Plastic hinge length need not be defined in this model and graded damages can be monitored using strain limit states at different levels across the section and along the member [Jiang, *et al.*, 2011].

**(c) Strut and Tie Model**

In this model, the strut and tie concept typically used to model deep beams, shear walls, and other elements are followed to investigate elastic and post-cracking plastic behaviour. Structural wall is assumed to resist lateral loads by forming tension-compression struts as a couple, and shear by diagonal elements, like in a truss. But, the strut and tie model is challenging for adoption in wider walls or walls with several panels [Panagiotou, *et al.*, 2012].

**(d) Shell Model**

In this model, long and complex structural walls are modeled using shell finite elements. Using layered shells, multi-layer models multiple layers of concrete and reinforcement can be modelled. But, when a shell element is subjected to in-plane stresses and deformation, the complex stress state and presence of reinforcement in any arbitrary direction with regard to the natural coordinates of shell element offer challenges in establishing a nonlinear force-deformation relationship. Thus, this model is not commonly adopted to model structural walls. [Anwar, *et al.*, 2009].

The following section discusses the most suitable option in commercial software PERFORM 3D which is used in this thesis work.

#### *2.5.2.1 Inelasticity in structural walls in PERFORM 3D*

Fiber modeling can be used in PERFORM 3D to model structural walls. Elastic and inelastic cross-sections of concrete and reinforcing fibre segments can be used to define wall components [CSI,2018]. Graded damages in walls are monitored of select fibres by defining strain limit states; wall is divided into a finite number of fibre segments, with vertical reinforcement specified at the center of the cross-section (Figure 2.11).

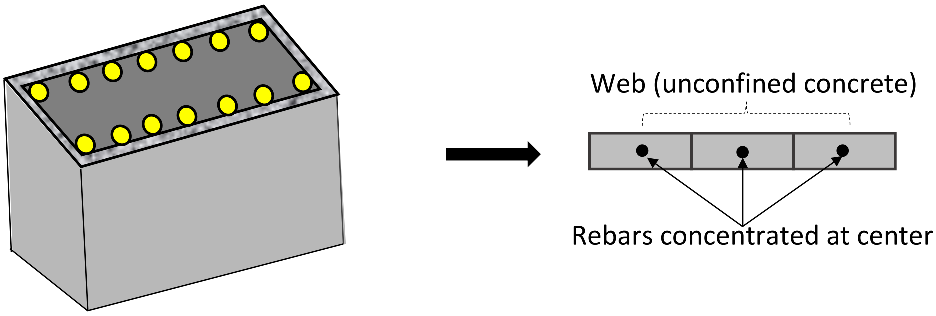


**Figure 2.11**: Fiber modelling of structural wall in PERFORM 3D

Confined concrete model is defined for boundary elements, and unconfined concrete for wall web. Past literature recommends fiber modeling as one of the efficient methods to model structural walls and capture the nonlinear behavior of walls.
As the inelasticity of sections stems from the constitutive relationship of the constituent materials in cross-sections, the following section discusses the constitutive relations commonly adopted, and later used for input for the work carried out for this thesis.

## 2.6 CONSTITUTIVE MODELLING

Material property of RC sections are defined by stress-strain ($\sigma$-$\varepsilon$) relationship of concrete and reinforcement. A RC structural member comprises of confined concrete core, unconfined concrete cover, and reinforcement. When unconfined cover concrete is compressed longitudinally, the concrete will be in a uniaxial state of stress. When the applied axial stress reaches uniaxial strength, concrete attempts to expand due to progressive internal fracturing. Transverse reinforcement resists this, and concrete restrained in a direction perpendicular to the applied stress is defined as confined concrete. Confinement of concrete by transverse reinforcements in RC sections increases the limits of maximum compressive stress and compressive strain in concrete. Thus, concrete confinement models are used to define core concrete, and concrete unconfined models for cover concrete. Mander's confinement model is used in this study to define $\sigma$-$\varepsilon$ relationship of both unconfined and confined concrete [Mander, *et al*., 1988]. Further, $\sigma$-$\varepsilon$ relationship of reinforcement available in published literature is used in this study.

### (a) Stress-strain curve of concrete as per Mander Model

Figure 2.12 schematically represents the Mander's confinement model. This model is applicable to both circular and rectangular RC sections. In this study, the maximum strain in concrete is limited to the strain corresponding to a drop in 20% of peak strength [Sunitha, 2017]. The calculation of $\sigma$-$\varepsilon$ values can be determined using the following:

$$f_c = \frac{f'_{cc} x r}{r - 1 + x^r}, \tag{2.2}$$

where $x = \frac{\varepsilon_c}{\varepsilon_{cc}}$; (2.3)

$$\varepsilon_{cc} = \varepsilon_{co}\left[1 + 5\left(\frac{f'_{cc}}{f'_{co}} - 1\right)\right]; \tag{2.4}$$

$$r = \frac{E_c}{(E_c - E_{c,sec})}; \text{ and} \tag{2.5}$$

$$f'_{cc} = f'_{co}\left(-1.254 + 2.254\sqrt{1 + \frac{7.94 f'_l}{f'_{co}}} - 2\frac{f'_l}{f'_{co}}\right). \tag{2.6}$$

Maximum strain capacity of confined concrete is assumed to correspond to fracture strain of transverse reinforcement [Paulay and Priestely, 1992], and can be estimated as:

$$\varepsilon_{c,max} = 0.004 + \frac{1.4\rho_s f_{yt}\varepsilon_{su}}{f'_{cc}}. \tag{2.7}$$

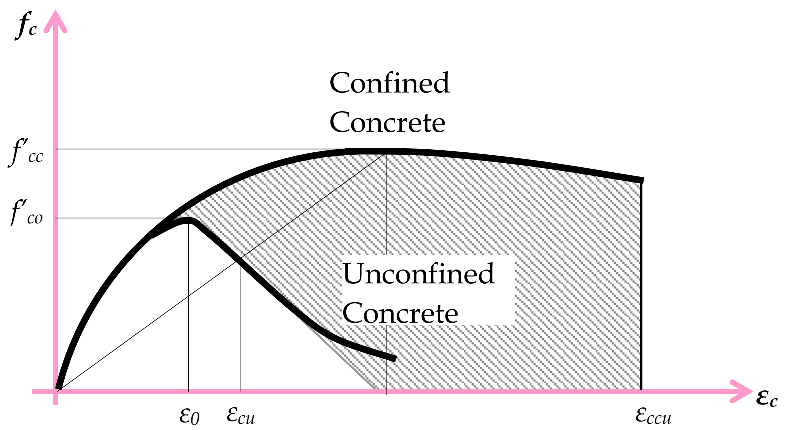


**Figure 2.12**: Stress-strain curve of concrete

### (b) Stress- strain curve for reinforcement

Of the many stress-strain models available for reinforcement, the curve considered in this study comprises of two parts: (a) linear elastic part up to the characteristic yield stress $f_y$ and strain 0.002+($f_y/E_s$), and (b) linear plastic part up to $f_y$ and strain 0.12 (Figure 2.13) [Sunitha, 2017; Deshmukh, 2017]. In general, 17- 25% strain hardening can also be considered in reinforcement [Rai, *et al*., 2012].

## 2.7 GAP AREAS

Based on the review of literature pertaining to seismic behaviour of structural systems, and in particular of hospital buildings, following gap areas are identified:

(1) Use of wall-frame structural systems for achieving better seismic performance is recommended in comparison to that achievable with moment resisting frames. But, it has been observed from past earthquake experience that wall-frames also exhibit inadequate seismic performance. Therefore, there is an urgent need to investigate the seismic performance of wall-frames to meet a preferred performance;

(2) Improper placement of structural walls in the structural plan has been identified as a contributing factor to the collapse of structures. Thus, it is imperative to verify the proper positioning of structural walls in wall-frame systems;

(3) Hospital building collapses during earthquakes are unacceptable. There is a need to confirm the adequacy of available design guidelines for hospital design and further complement them with additional recommendations;

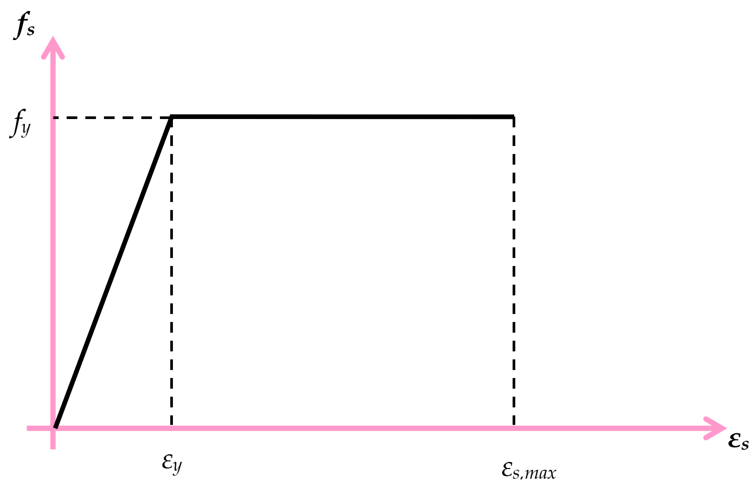


**Figure 2.13**: Stress-strain curve of reinforcement

(4) Structural systems suitable for hospital buildings are not available in design codes. Numerical investigations incorporating guidelines available in special documents need to be conducted to validate and quantify their efficacy; and

(5) Earthquake being displacement loading, a proposal need to be provided for estimation of approximate deformation demands imposed on typical hospital buildings, and guidelines to meet the preferred *Occupiability* performance objective be recommended.

## 2.8 OBJECTIVES AND SCOPE OF PRESENT STUDY

Based on the gap areas identified, the salient objectives of the present study are:

(1) To investigate, evaluate and quantify *seismic demands* on wall-frame buildings;

(2) To quantify *limiting structural damage*s in hospital buildings to meet *Occupiability* performance objectives; and

(3) To recommend *structural configuration, structural plan density* and *design parameters* required to meet *Occupiability* performance objective in wall-frame hospital buildings.

The present study is limited to hospitals with RC wall-frame structural system with regular structural grid. Unreinforced masonry infills are not considered in numerical modelling. Soil structure interaction is not included. No damage is expected in beam-column joints; beam-column joints are assumed to be infinitely stiff and strong. Members are designed to respond predominately in flexure; shear failure is precluded by following capacity design criteria.

...

*Blank Page*

# 3

# Effects of Configuration and Location of Structural Walls on Seismic Behaviour of Wall-Frame Systems

## 3.0 OVERVIEW

*Essential virtues* of earthquake resistant structures are:

(1) Good *structural configuration*, (2) Minimum initial *lateral stiffness*, (3) Minimum *lateral strength*, (4) Adequate *ductility*, and (5) Desirable *collapse mechanism* [Murty, *et al*., 2012; Vijaynarayanan, *et al*., 2022].

Of the above, if the design starts with a good structural configuration, namely (a) orientation, (b) location, and (c) sufficient number of lateral load resisting elements, the rest of the virtues are easy to implement as per preferred behaviour of structures. In this chapter, firstly, pilot numerical studies on 2D wall frames are performed to investigate contribution of *wall-plan aspect ratio* on the inelastic behaviour. Nonlinear static and nonlinear dynamic analyses results are used to infer the suitable wall-plan aspect ratio. For the purpose, limit states of structural damages are defined and monitored. Secondly, to confirm 2D seismic demands and obtain more realistic demand estimates, numerical studies on 3D structures are carried out to obtain the performance. In total seven 3D buildings (A–G) are considered, and their linear behaviour corrected to obtain translation modes of oscillation.

## 3.1 MATERIAL CONSTITUTIVE LAW

Steel and concrete grades assumed are M30 and Fe415 respectively (Section 2.5). Concrete confinement model recommended by Mander is followed and the nonlinear concrete stress-strain curve idealized for use as input in PERFORM3D. For the idealization, Mander stress-strain curve until a drop in 20% strength is considered (Park and Paulay, 1975). Fe415 grade reinforcement is used to develop stress-strain curve in three parts (Figure 3.1). They are a linear part up to characteristic yield stress $f_y$, secondly a linear part up to ultimate strength of 1.17 $f_y$ (assuming 17% strain hardening) [Rai, *et al.*, 2012] and thirdly a dropping linear part up to 50% ultimate strength [Inel M. and Ozmen H B., 2006].

## 3.2 LIMIT STATES OF STRUCTURAL DAMAGE

Five distinct strain limit states based on material constitutive relationship are defined for monitoring structural damages in study frames. The limiting strain values and select schematic representations are presented below (Figures 3.2—3.4):

(1) Yielding of first layer of longitudinal reinforcement in *beams or columns* in tension at limiting yield strain ($\varepsilon_y$) of 0.002+($f_y/E_s$);

(2) Yielding of first layer of vertical longitudinal reinforcement in *structural walls*, in tension at limiting yield strain ($\varepsilon_y$) of 0.002+($f_y/E_s$);

(3) Crushing of extreme fibre of confined concrete in compression in beams, at limiting confined strain ($\varepsilon_{ccu}$) obtained from Mander model;

(4) Crushing of extreme fibre of confined concrete in compression in columns at limiting confined strain ($\varepsilon_{ccu}$) obtained from Mander model; and

(5) Spalling of extreme fibre of unconfined concrete in compression in structural walls at limiting unconfined strain ($\varepsilon_{cu}$) of 0.0035.

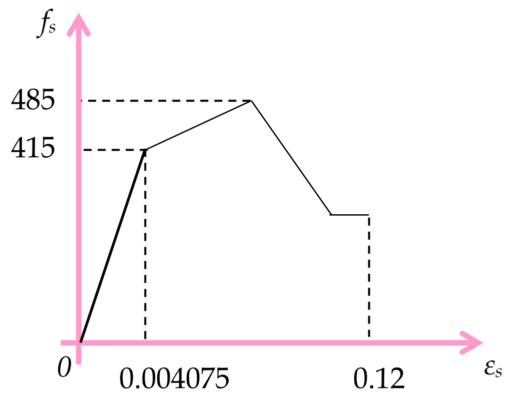


**Figure 3.1**: Stress-strain relation of reinforcement used in the study

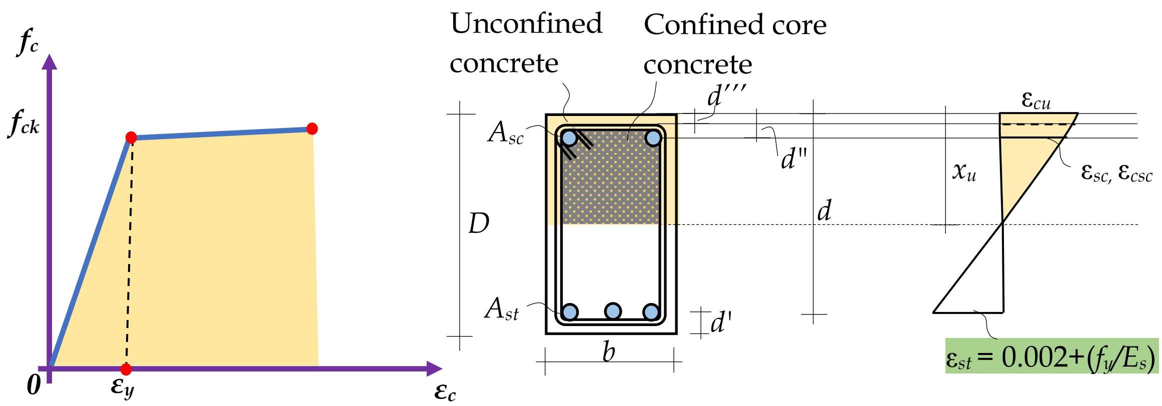


**Figure 3.2**: Limit state of yielding of reinforcement in structural elements

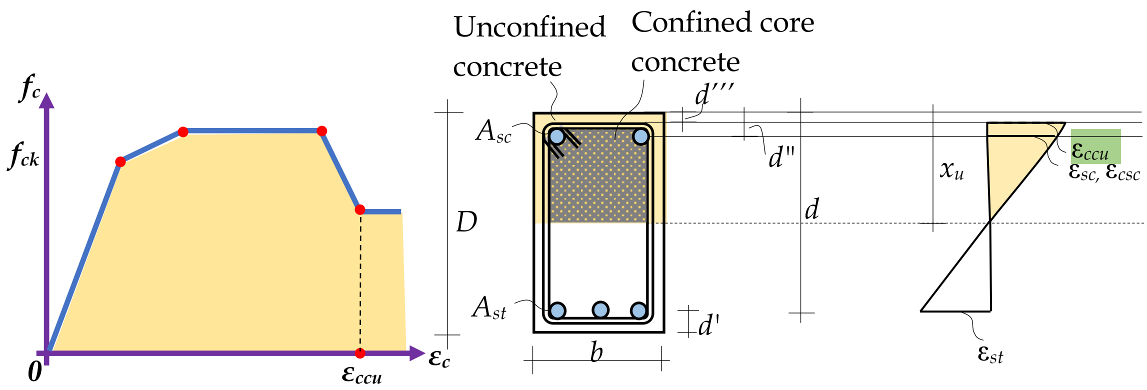


**Figure 3.3**: Limit state of crushing of *confined* concrete in beams and columns

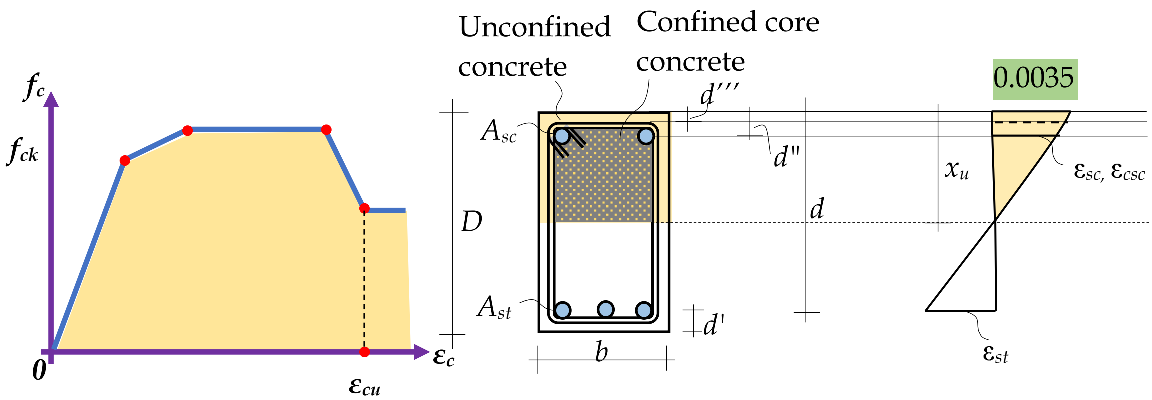


**Figure 3.4**: Limit state of crushing of *unconfined* concrete in structural walls

### 3.3 NUMERICAL STUDY ON 2D WALL-FRAMES WITH VARYING WALL-PLAN ASPECT RATIO

The study wall-frame is 6-storey with typical storey height 3 *m*, 3 bays with bay length 6 *m* at ends (Figure 3.5). Six different numerical models with structural wall thickness 250 *mm*, and wall plan-aspect ratios (length of the wall/thickness of wall) 4, 8, 12, 16, 20 and 24 are considered. Slab (125 *mm* thick) loads, and brick masonry infill (unit weight 18$kN/m^3$) loads are distributed on beams. Live load considered is 3$kN/m^2$. Seismic loads are estimated using IS1893 2016. Design and detailing are performed as per Indian Standard codes [IS456 2000; IS13920 2016]. Reinforcement details of structural elements of study wall-frames are listed in Appendix A. Nonlinear static and dynamic analyses are performed in commercial structural analysis software PERFORM 3D [CSI 2018].

Further, to model inelasticity plastic zone model is adopted for defining inelasticity in beams, and columns (Figure 2.9(a)). Plastic zones are modeled using fiber sections, while the middle portion of the beam and columns are assumed elastic (Section 2.4) (Figure 3.6). Plastic hinge length considered is 0.5*D*, where D is overall depth of section (Section 2.4.1.1). Fiber inelasticity is used in structural walls, fibres are defined across the height in structural walls (Section 2.4.2.1) (Figure 2.9).

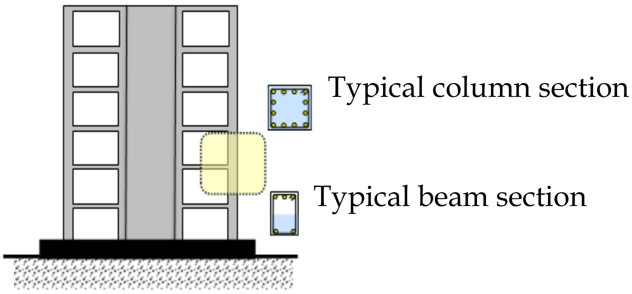


**Figure 3.5**: Elevation of Study Wall-Frame

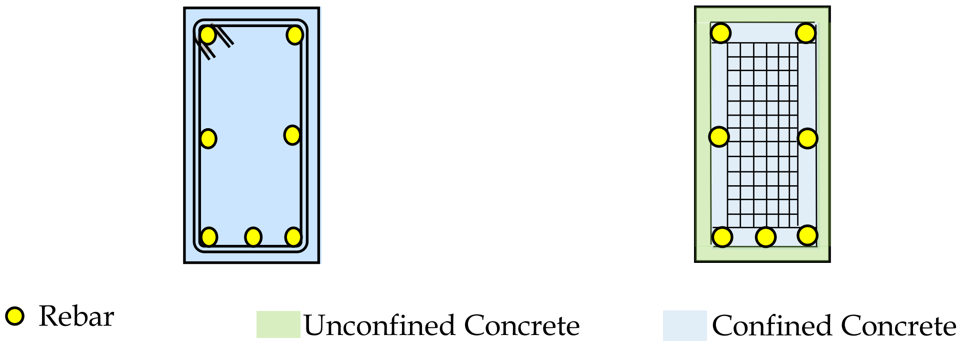


**Figure 3.6**: Fibres in RC cross-section

## 3.4 DISCUSSION OF RESULTS

For all study frames, the dynamic properties of frames are investigated by first performing modal analysis. The evaluation of damages in wall-frames corresponding to different limit states is evaluated by performing *NSA* and *NTHA*. All study frames are observed for additional drift parameters, namely overall drift, storey drift, and yield drift. The subsequent section presents an analysis of the outcomes obtained from various investigations.

### 3.4.1 Modal Analysis

Fundamental periods of study wall-frames are tabulated in Table 3.1. The fundamental period of the wall-frame decreases with increase in wall plan-aspect ratio. This can be attributed to increase in stiffness, due to increasing stiffness of the structural walls.

Further, to investigate the virtues of earthquake resistant buildings, *NSA* is performed. Alongside, damages incurring in frames at salient drifts are noted.

### 3.4.2 Nonlinear Static Response

Displacement-controlled nonlinear static analyses are performed of study wall-frames and nonlinear responses investigated.

***(a) Observations from monitored limit states of structural damage***

Five strain limit states (Figures 3.2-3.5) are monitored to represent structural damages (Figure 3.7). In study wall-frames with wall plan-aspect ratio 4 and 8, while yielding of reinforcement occurred first in beams, yielding of reinforcement occurred first in structural walls in other wall-frames. This can be attributed to the increase in stiffness of structure with wall plan-aspect ratio.

**Table 3.1:** Fundamental period of study wall-frames.

| *Wall plan-aspect ratio* | *Fundamental Period (sec)* |
|---|---|
| 4 | 1.39 |
| 8 | 0.85 |
| 12 | 0.46 |
| 16 | 0.40 |
| 20 | 0.29 |
| 24 | 0.22 |

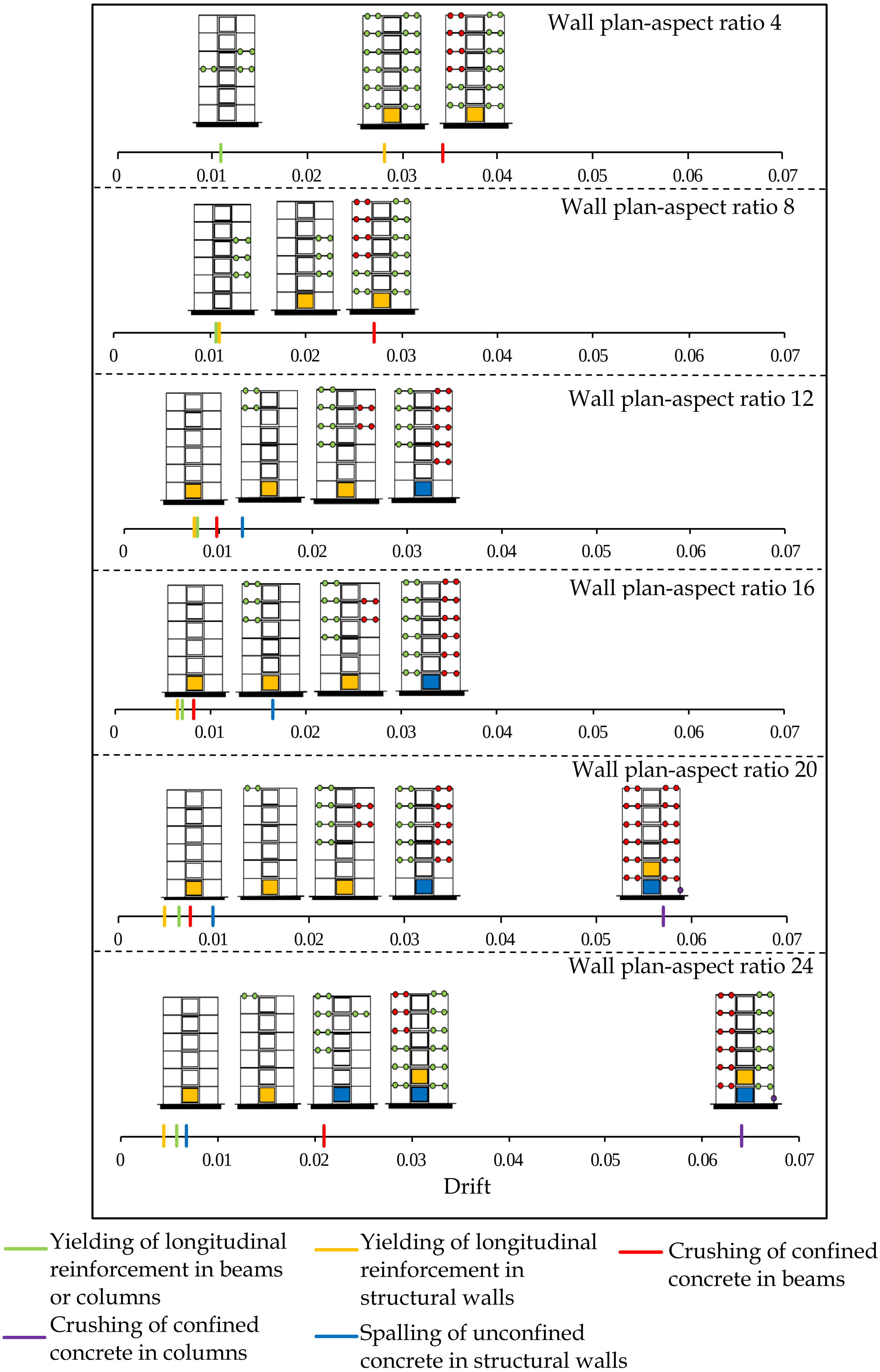


**Figure 3.7:** Limit states of structural damages incurred

Further, damage occurred at the base of the columns in wall-frames having wall plan aspect ratio 20 and 24. And, extent of damages accrued in structural walls increased with increase in wall plan-aspect ratio.

***(b) Nonlinear static response curves***

Normalized pushover curves of the 6 wall-frames are presented (Figure 3.8); the base shear $H$ of each structure is normalized with maximum lateral strength $H_{max}$ and the lateral deformation $\delta$ by maximum deformation $\delta_{max}$. Limit states representing the beginning of structural damages in different structural components are mentioned at salient drifts. Further, a single multi-linear pushover curve using the average normalized strength and average normalized deformation corresponding to the different limit states of structural damages demonstrate that the limit states occur in wall-frames at similar drifts (Figure 3.9) [Sunitha, P., 2017]. Here, the nonlinear static response of wall-frame with wall plan-aspect ratio 4 is not used as the lateral behavior at first yielding is significantly different from other cases (Figure 3.7).

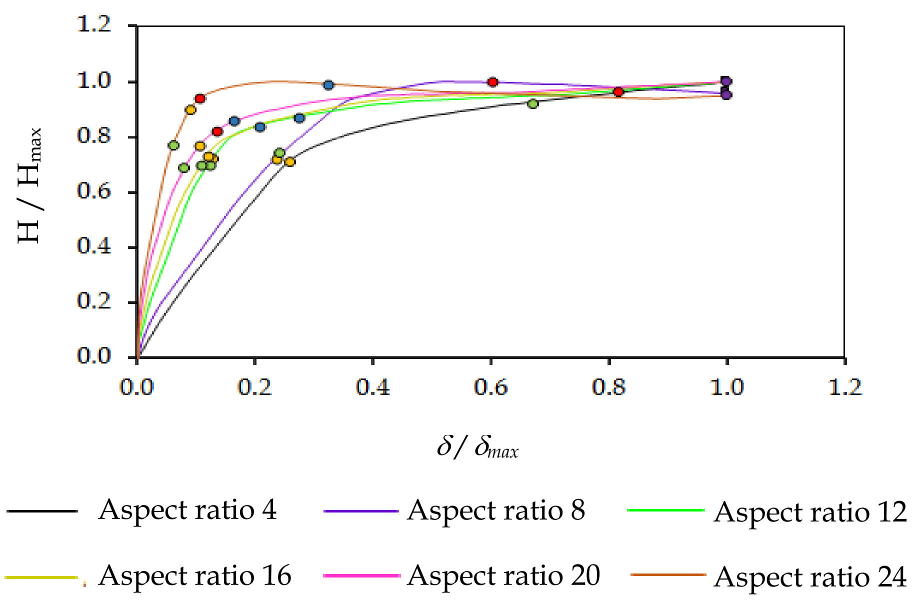


**Figure 3.8:** Normalized static response curves & limit states of structural damage in study wall-frames

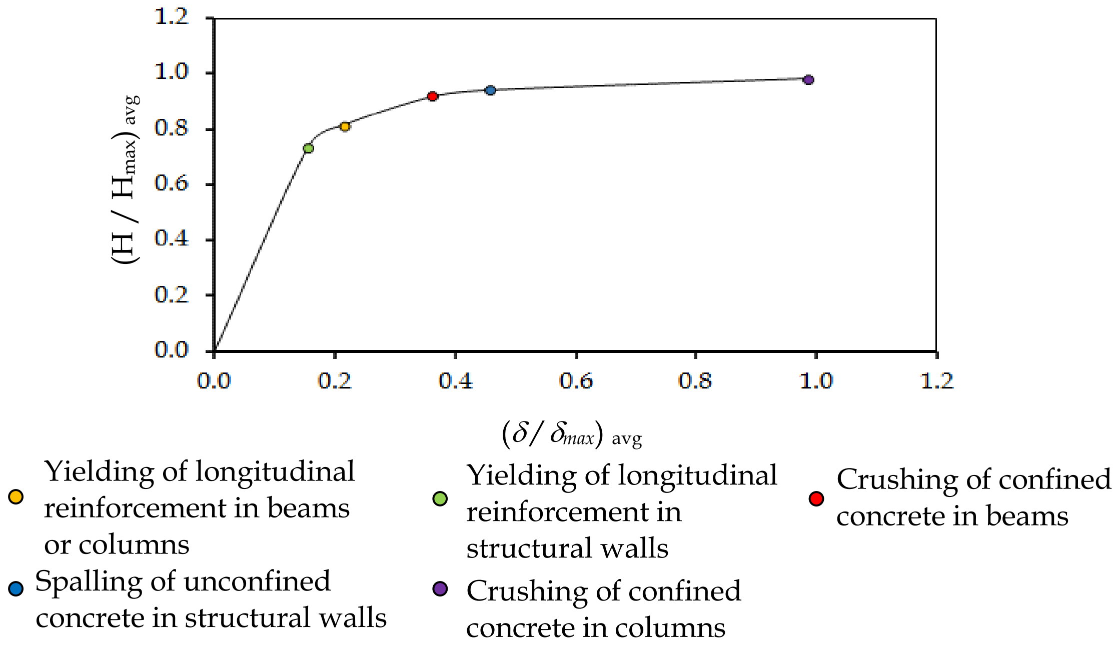


**Figure 3.9:** Renormalized nonlinear static response curve

#### *3.4.2.1 Estimation of earthquake resistant virtues of study frames*

Earthquake resistant virtues, namely lateral stiffness, lateral strength (represented by overstrength here) and lateral ductility of wall-frames is estimated by idealizing the pushover curves following energy balance criteria under idealized and nonlinear curves [ASCE/SEI 41-17, 2017]. Overstrength ($\Omega$) is estimated as the ratio between maximum lateral strength and design lateral strength (Table 3.2).

##### *3.4.2.1 (a) Lateral stiffness, ductility, and deformability*

The lateral stiffness increased, overstrength reduced with increase in wall plan-aspect ratio; higher overstrength in wall-frames with low wall plan-aspect ratio can be attributed to predominant gravity loads [Navin and Jain, 1995]. Nevertheless, an increase in overstrength is also observed after the initial reduction, especially in frames with wall plan-aspect ratio 20 and 24. Ductility capacity remained constant in wall-frames with low wall plan-aspect ratio, but increased for wall-frames with higher wall plan-aspect ratios. This may be due to the increased stiffness leading to early yielding in these wall-frames, and the increase in lateral resistance to sustain high lateral deformation demands.

**Table 3.2:** Earthquake resistant virtues of study wall-frames

| *Wall plan-aspect ratio* | *Stiffness (kN/m)* | *Overstrength* | *Ductility* |
|---|---|---|---|
| 4 | 1389 | 7.05 | 3.63 |
| 8 | 2184 | 5.6 | 3.66 |
| 12 | 5762 | 5.02 | 4.48 |
| 16 | 7014 | 4.20 | 9.55 |
| 20 | 10450 | 4.20 | 12.97 |
| 24 | 17050 | 5.31 | 13.80 |

### 3.4.3 Nonlinear Dynamic Analysis

Nonlinear time history analysis (*NTHA*) is also performed on the 6-study wall-frames using 10 natural ground motions (Table 3.3) whose acceleration response spectrum is shown in Figure 3.10. Spectral amplitude scaling is adopted at elastic natural period of the building (Section 2.3.1) (Figure 3.11). Storey drifts obtained from *NTHA* demonstrate significant drift capacity in all wall-frames; flexible wall-frames have more drift capacity compared to stiffer wall-frames. Further, drift demand imposed in lower storeys is about 1% in wall-frames with wall plan-aspect ratios 24, 20,16, and 12, while in wall-frames with lower aspect ratios, it is significantly more than 1%.

**Table 3.3:** Details of ground motions

| *No.* | *Event* | *Station* | *Year* | $M_w$ | *PGA (g)* | *Epicentral distance (km)* |
|---|---|---|---|---|---|---|
| 1 | Chi Chi | TCU 006 | 1999 | 6.2 | 0.41 | 126.09 |
| 2 | Imperial Valley | Coachella Canal #4 | 1979 | 6.5 | 0.11 | 49.30 |
| 3 | Loma Prieta | Hollister South Pine | 1989 | 6.9 | 0.36 | 48.24 |
| 4 | Chi Chi | KAU 057 | 1999 | 7.6 | 0.34 | 146.78 |
| 5 | Kern County | Taft | 1952 | 7.3 | 0.01 | 36.89 |
| 6 | Uttarkashi | Bhatwari | 1991 | 6.8 | 0.25 | 36.00 |
| 7 | Fruili | Tolmezzo | 1976 | 6.4 | 0.35 | 28.00 |
| 8 | Hollister | USGS STATION 1028 | 1961 | 5.5 | 0.20 | 18.92 |
| 9 | Imperial Valley | USGS STATION 5115 | 1979 | 6.5 | 0.28 | 2.47 |
| 10 | Kobe | KAKOGAWA (CUE90) | 1995 | 6.9 | 0.34 | 22.50 |

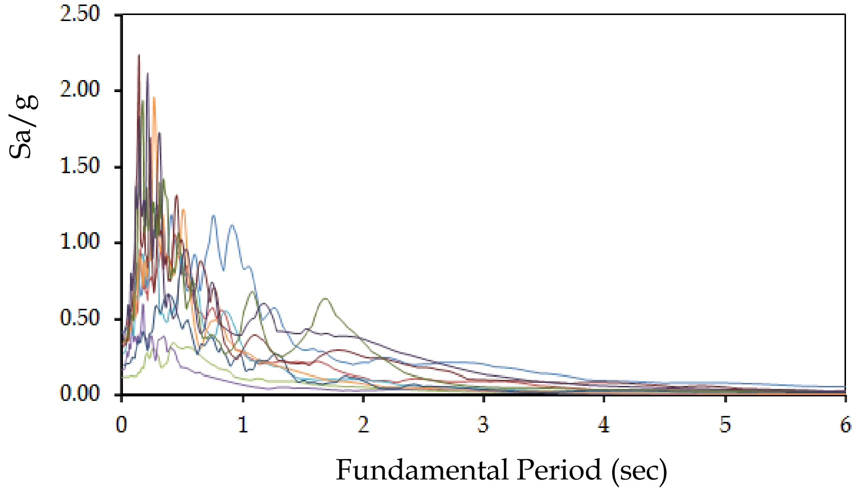


**Figure 3.10:** Acceleration response spectrum of ground motion used in the 2D wall-frame study

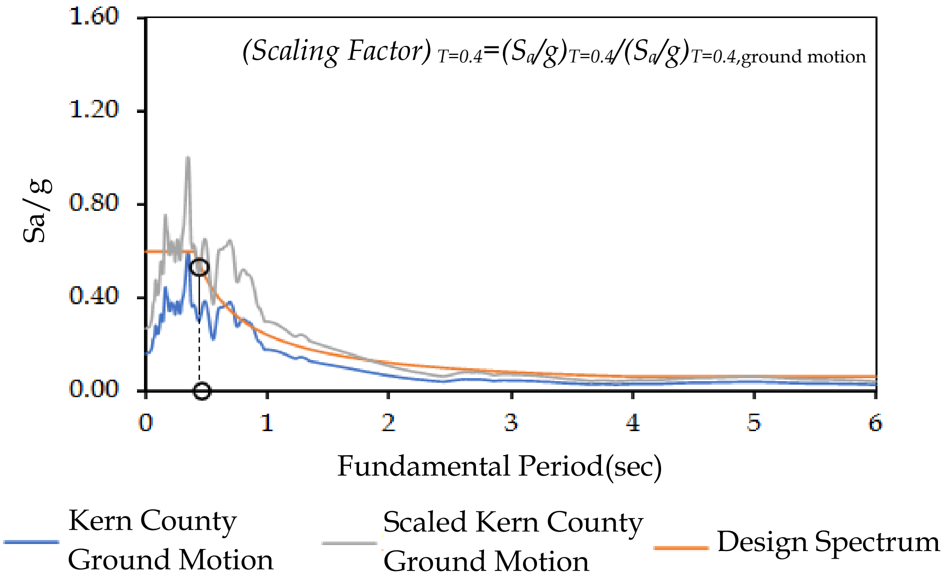


**Figure 3.11:** Scaling of Kern County Ground Motion

### 3.4.4 Comparison of NSA and NTHA Lateral Deformation Behaviour

Maximum drift demands imposed during *NTHA* and *NSA* are compared (Figure 3.12). For the purpose, ultimate drift from nonlinear static analysis and maximum drift from time history analysis under each ground motion are monitored. In most wall-frames, maximum drift demand imposed during *NTHA* are lower than the corresponding maximum drift obtained from *NSA* [Sunitha, *et al.*, 2021]. Thus, the results from NSA are reasonably accurate to predict the seismic behaviour of the considered wall-frames. But,

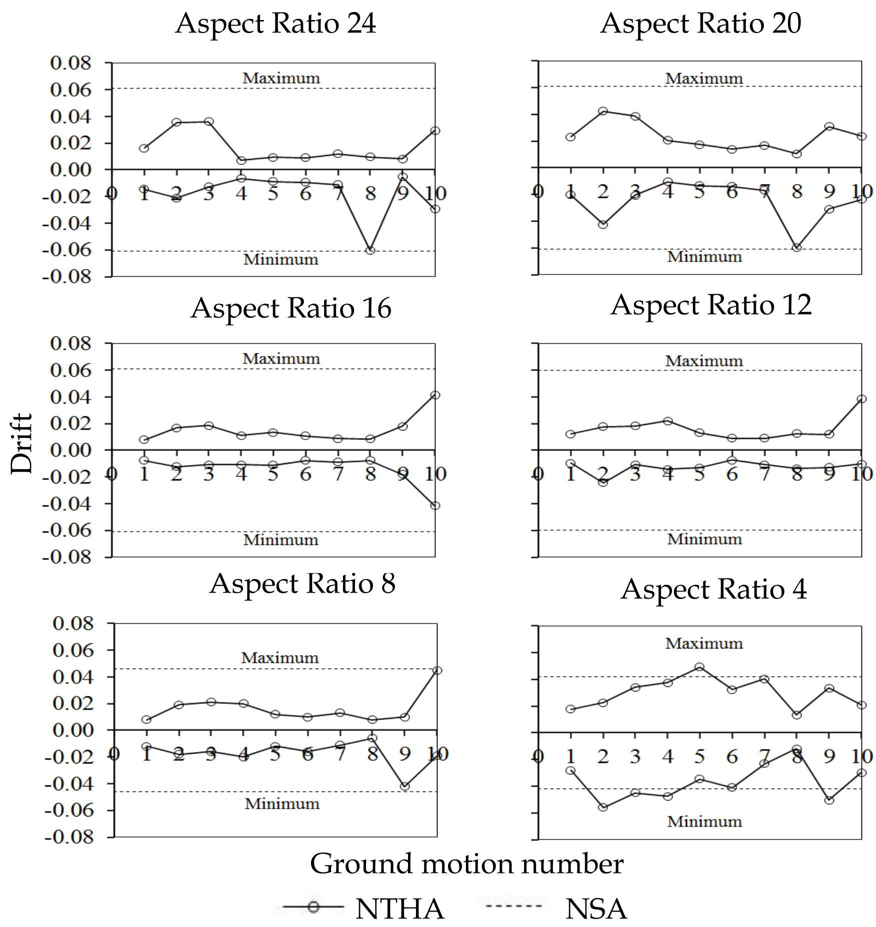


**Figure 3.12:** Overall drift of study wall-frames

in wall-frame with wall plan-aspect ratio 4, under Imperial Valley, Kern County, Chi Chi and Loma Prieta GM, drift demand exceeded that from *NSA*.

Further, percentages of design drift, yield drift, and elastic maximum drift for all structures are estimated (Table 3.4) (Figure 3.13). Here, elastic maximum drift is assumed to be the drift demand imposed in the structure if the structure were to remain elastic as per equal displacement rule [Housner and Jennings, 1982]. With increase in wall plan-aspect ratio, yielding occurred early due to higher stiffness in these wall-frames. Also, it is observed that first yielding of reinforcement in structural members occurred after meeting the elastic maximum drift. This behaviour can be crucial for lifeline structures like hospitals for the required post-earthquake performance of continuous functionality.

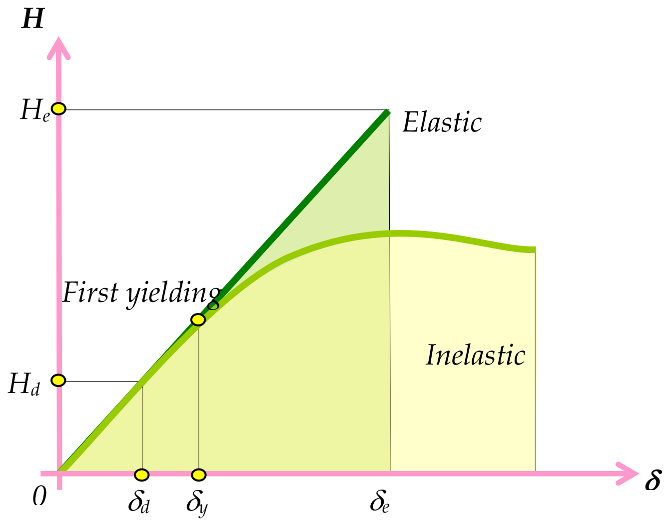


**Figure 3.13:** Schematic diagram of elastic maximum drift ($\delta_e$), yield drift ($\delta_y$) and design drift ($\delta_d$)

Numerical studies using ground motion data is carried out conclude the behaviour. Also, drift corresponding to first yield from *NSA* and *NTHA* are also compared (Table 3.5). In all wall-frames, except with wall plan-aspect ratio 4, drift values corresponding to first yielding in wall-frames during *NTHA* are less than that obtained from NSA. Further, these drift values (demands) from *NTHA* are also lower than the elastic maximum drift (Table 3.4); this is an indication that damages start accruing in the wall-frames before meeting the elastic maximum drift demands, as obtained from *NSA*.

But, the maximum elastic drift demand from NSA of study wall-frames is not met before first yielding of structural members during *NTHA*, thereby not clearly confirming the occupiability of these structures. This behavior should be verified by performing *NTHA* using more natural ground motions on 3D wall-frame structures commonly recommended for hospital structures; recommendation on earthquake resistant features for occupiability of hospital buildings must be based on more numerical investigations. Hence, further investigations are carried out on 3D structures mainly hospital structures here after in Chapter 4.

**Table 3.4:** Salient drifts in study wall-frames from NSA

| *Wall plan-aspect ratio* | *Design* | *Drift (%) First Yield* | *Elastic Maximum* |
|---|---|---|---|
| 4 | 0.17 | 1.09 | 0.85 |
| 8 | 0.15 | 1.07 | 0.75 |
| 12 | 0.12 | 0.75 | 0.60 |
| 16 | 0.11 | 0.65 | 0.55 |
| 20 | 0.065 | 0.48 | 0.325 |
| 24 | 0.019 | 0.44 | 0.095 |

**Table 3.5**: Drift corresponding to *first yielding* in study wall-frames from NSA & NTHA

| **Aspect ratio** / **Ground motion** | **4** | **8** | **12** | **16** | **20** | **24** |
|---|---|---|---|---|---|---|
| | Drift | | | | | |
| **1** | 0.0040 | 0.0058 | 0.0045 | 0.0049 | 0.0024 | 0.0040 |
| **2** | 0.0044 | 0.0100 | 0.0072 | 0.0059 | 0.0040 | 0.0042 |
| **3** | 0.0091 | 0.0093 | 0.0047 | 0.0061 | 0.0019 | 0.0044 |
| **4** | 0.0255 | 0.0058 | 0.0072 | 0.0063 | 0.0042 | 0.0038 |
| **5** | 0.0094 | 0.0087 | 0.0069 | 0.0047 | 0.0032 | 0.0040 |
| **6** | 0.0250 | 0.0100 | 0.0042 | 0.0063 | 0.0010 | 0.0039 |
| **7** | 0.0021 | 0.0045 | 0.0052 | 0.0059 | 0.0039 | 0.0036 |
| **8** | 0.0094 | 0.0070 | 0.0067 | 0.0064 | 0.0030 | 0.0021 |
| **9** | 0.0010 | 0.0073 | 0.0057 | 0.0039 | 0.0035 | 0.0041 |
| **10** | 0.0014 | 0.0100 | 0.0071 | 0.0060 | 0.0046 | 0.0038 |
| **NSA** | 0.0109 | 0.0107 | 0.0075 | 0.0065 | 0.0048 | 0.0044 |

## 3.5 LINEAR ELASTIC BEHAVIOUR STUDY ON 3D WALL-FRAME STRUCTURES WITH VARYING SPD OF STRUCTURAL WALLS

The study building is a hospital located in Seismic Zone IV and founded on soft soil. To reduce variabilities in numerical modelling, the original plan is slightly resized to a regular grid and columns are arranged concentrically (Figure 3.14). Rigid diaphragms are assumed, and slabs are not modelled. Analysis, design, and detailing are carried out as per Indian Standards [IS456, 2000; IS1893 (1), 2016; IS13920, 2016]. 7 structural configurations are considered (Buildings A—G), and linear elastic performance examined in PERFORM 3D. The changes adopted in structural grid are shown in each plan and marked in red (Figure 3.15). Cross-section and design details of structural members are provided in Appendix A.

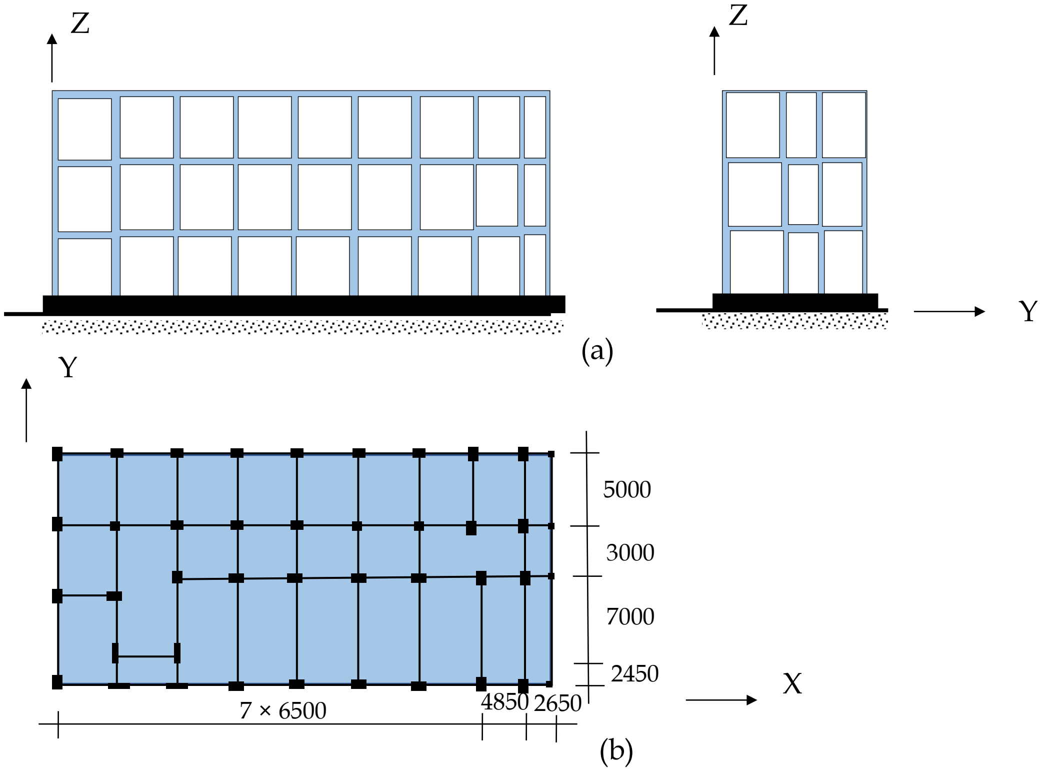


**Figure 3.14**: Original Study Building A, (a) Elevation, (b) Plan

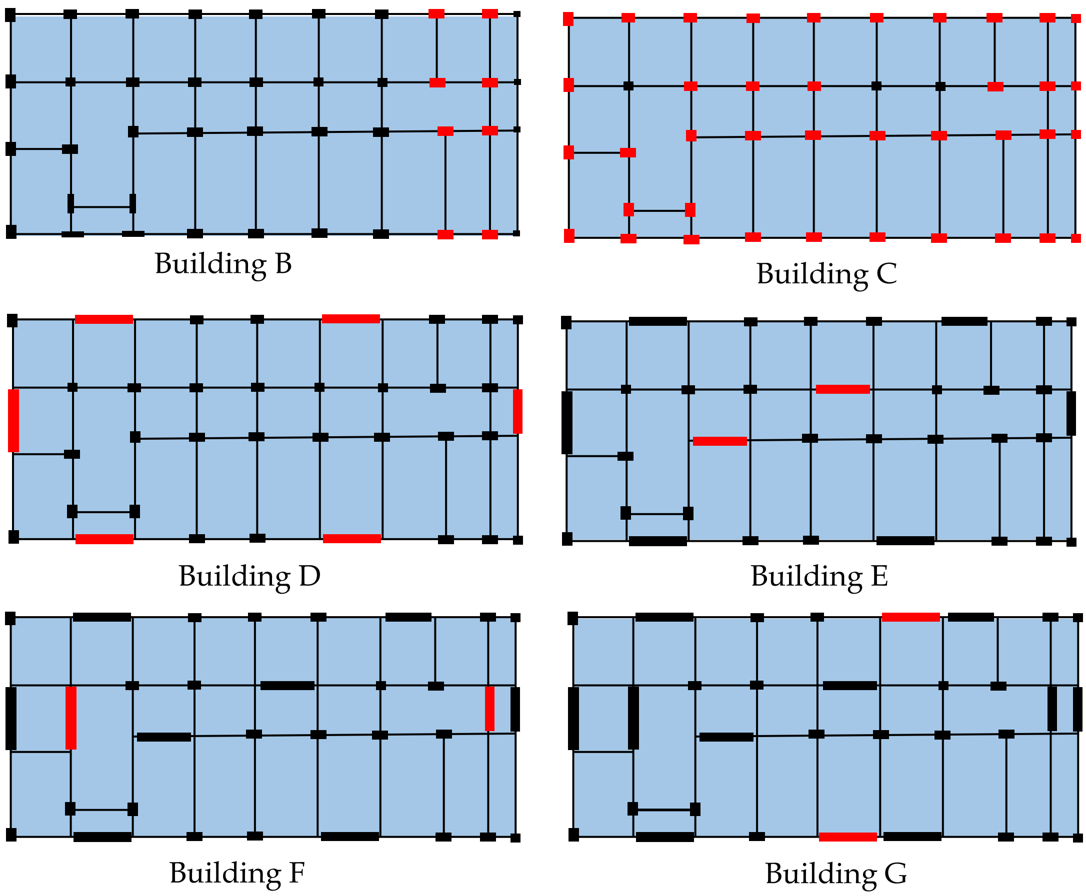


**Figure 3.15**: Structural configurations considered for numerical investigations

In addition, the location and orientation of lateral load-resisting elements is crucial for the seismic performance of structures. The orientation of columns and structural walls in the study buildings B–G is adjusted to eliminate undesirable oscillation modes and vertical irregularities. The following section discusses the above effects.

### 3.5.1 Effect of orientation and location of lateral load resisting members

The fundamental mode is preferably translational in both principal plan directions of structures. In the case of Building A, the fundamental mode of oscillation is torsional. Thus the orientation of marked columns (Figure 3.16) was changed to bring translational mode along principal axis (Figure 3.16). Further, the location of structural walls affects the overall stiffness, strength and largely stability of the structure. Thus the walls in rest of the buildings are carefully provided until stable linear behaviour is obtained. For example, providing structural walls as presented in Figure 3.17(a) demonstrated unstable linear behaviour of structure. On the other hand, distributed structural walls as in Figure 3.17(b) demonstrated stable linear behaviour. In the case of Building E, F and G overcrowding of structural walls are avoided.

### 3.5.2 Location of Centre of Mass and Centre of Resistance

The static eccentricity($e_{si}$) of a structure is determined as the distance between its Centre of Mass (*CM*) and Centre of Resistance (*CR*). In order to avoid torsional irregularity, static eccentricity should be minimized (Figure 3.18). To achieve the required SPD of structural walls for a given structure providing more structural walls will jeopardize the elastic and inelastic performance of building. This is due to the high

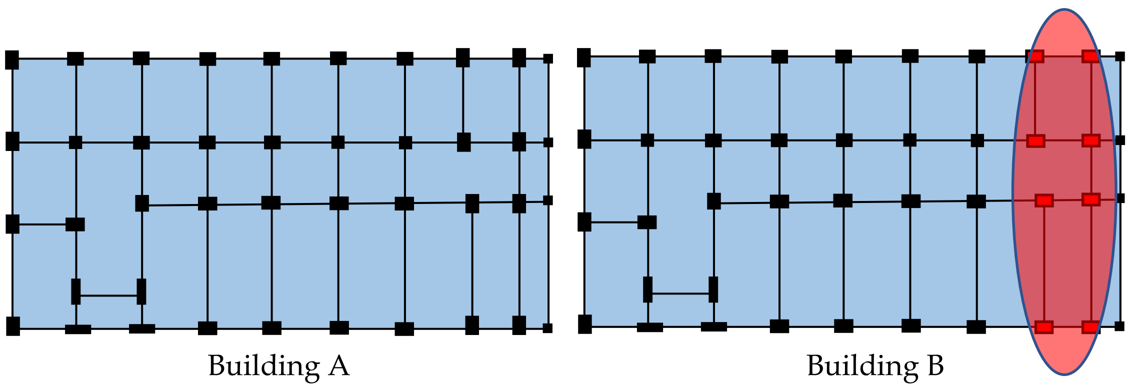


**Figure 3.16**: Importance of orientation of columns: Orientation of columns alters the mode of oscillation

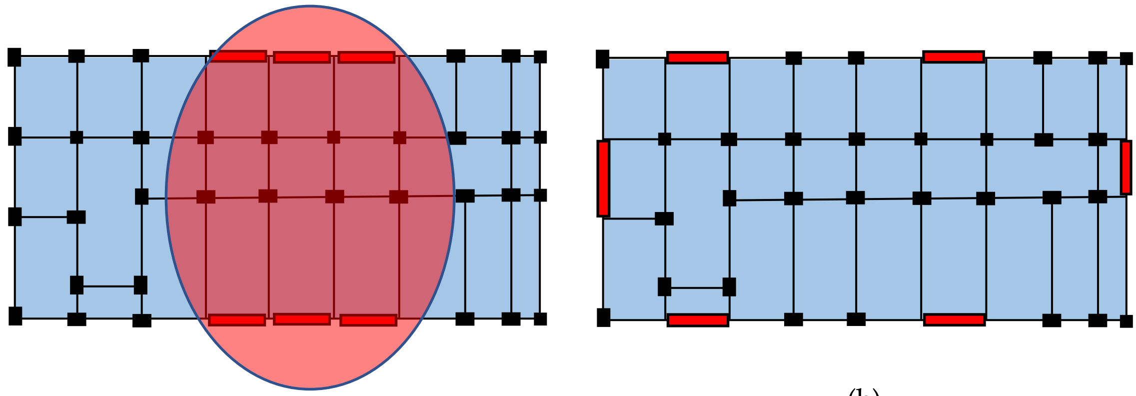

(a) (b)

**Figure 3.17**: Revising location of structural wall in Building D for improved behaviour

stiffness provided by structural walls. One solution to overcome this is to increase thickness of the wall without changing SPD of structural walls. Thus, it is recommended that walls should be positioned so that the centre of mass and the centre of resistance are not far apart. For example, in Building G with SPD of 4%, random configurations were first selected. *Modal analysis* is performed to examine the linear behaviour of structure, namely mode shape and fundamental period. It is observed that integral behaviour between walls and frames are absent, and excessive elastic deformations occurred in frames connected to walls. Secondly, the location of *CM* and *CR* are monitored (Table 3.6). In addition, 2 more alternate configuration are also considered for this study (Figure 3.19). For building G alternate configuration, distance between $CM_x$ and $CR_x$ is too far away. Thus, it should be avoided and structural plan having less eccentricity should be adopted. For Building F and alternate configuration of F, values of *CM* and *CR* are not too far away, but there is no integral behaviour of structural walls and moment frame members. It is observed that maximum static eccentricity for reasonably good behaviour is about 5 m.

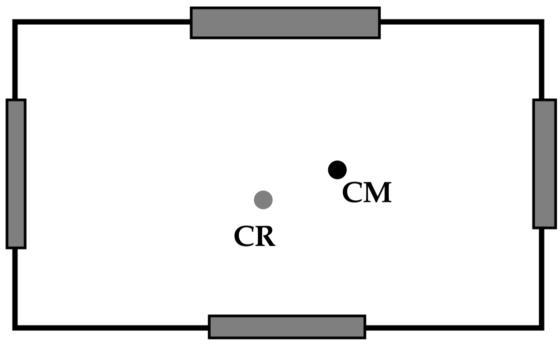


**Figure 3.18**: Schematic of *CM* and *CR* in a typical floor plan of  wall-frame building

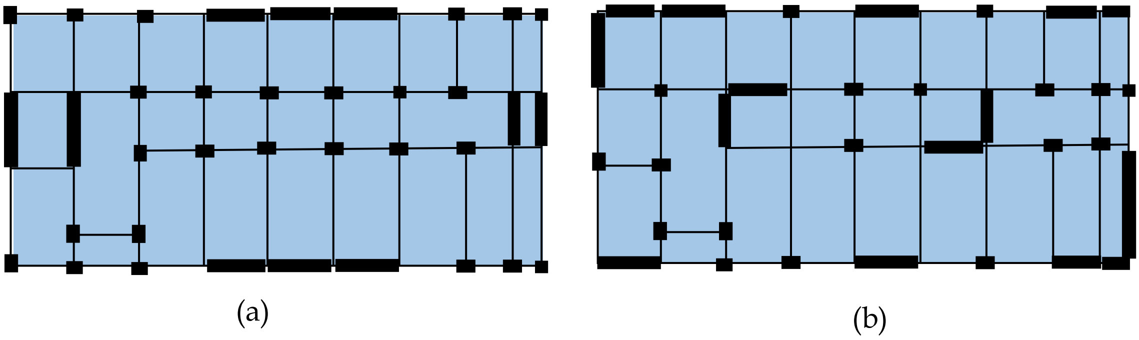


**Figure 3.19**: Alternate structural configuration of buildings: (a) F, and (b) G

**Table 3.6**: CM and CR of study buildings

| *Building* | *CM* | *CR* | *Static eccentricity* |
|---|---|---|---|
| A | (24.99,8.16) | (25.12,7.77) | (0.13, 0.39) |
| B | (24.99, 8.14) | (26.13, 7.72) | (1.14, 0.42) |
| C | (24.99, 8.14) | (26.13, 7.72) | (1.14, 0.42) |
| D | (25.03, 8.13) | (19.89, 7.46) | (5.14, 0.67) |
| E | (25.05, 8.11) | (19.07, 7.40) | (5.98 ,0.71) |
| F | (25.04, 8.10) | (19.00, 7.43) | (6.04, 0.72) |
| G | (25.31, 8.15) | (18.34, 7.27) | (6.97, 0.88) |
| F (Alternate) | (25.25,8.16) | (18.48,8.079) | (6.77,0.08) |
| G (Alternate) | (24.62, 8.19) | (36.22, 11.42) | (11.6,3.23) |

Apart from structural configuration, flexural strength ratio between column and beam should also be adequate such that desirable collapse mechanism is achieved. Thus, for study buildings A – C, CBSR is investigated and ensured to be designed with atleast 1.4 as recommended by IS 1893(1):2016.

### 3.6 Column-to-Beam Strength Ratio (CBSR (β))

CBSR (β) ratio is defined as the relative flexural strength between columns and beam framing into a joint. β values is evaluated of study buildings A, B, and C revised for with minimum 1.4. For building A and B, CBSR is less than 1, thus, Building C is designed for a minimum CBSR of 1.4 [IS 1893(1):2016] (Table 3.7).

**Table 3.7**: CBSR values of study building

| Building | CBSR Value |
|---|---|
| **A, B, C** | 0.8-1.4 |

## 3.7 CONCLUSIONS

Salient conclusions drawn from the work carried out as part of this Chapter are:

(1) Fiber-based inelasticity modeling help determine the virtues of earthquake resistant structures more realistically;

(2) Increasing the wall plan-aspect ratio provides reasonable lateral stiffness, lateral strength, and lateral ductility to sustain actual earthquakes;

(3) Wall-frames with high plan aspect ratio demonstrate significant lateral stiffness, ductility, drift capacity (minimum 3%);

(4) Wall-frames with wall plan-aspect ratio 4 is observed to be not suitable for use in hospital buildings because of higher seismic demands imposed and resulting poor seismic behaviour;

(5) Structural configurations are critical for achieving the preferred seismic performance of structures. The orientation of lateral load resisting members should be adjusted to prevent torsional mode; and

(6) Structural walls must be uniformly distributed in plan. It is recommended that, instead of using more number of structural walls, thicker structural walls be provided so that the static eccentricity is about 5 m.

...

# 4

# Numerical Study to Achieve Post-Earthquake Occupiability Performance

## 4.0 OVERVIEW

Earthquake Resistant Design (ERD) Philosophy allows graded structural damages in *normal* buildings [Murty *et al.*, 2012]. On the other hand, while ERD philosophy and allowable or graded damages in critical buildings like hospitals is unclear, such buildings are expected to remain occupiable after an earthquake. In view of the past earthquake behaviour of hospital buildings [Section 2.2.2], it is crucial to investigate elastic and inelastic behaviour by monitoring strain limit states of structural damages. This will help propose critical design parameters required for improving seismic safety of these buildings. This chapter presents numerical modeling procedure and elastic & inelastic responses of the study hospital building, designed and detailed as per Indian Standards. Recommendations on structural configurations, SPD, CBSR, and limit state of structural damage for preferred performance are arrived at for typical hospital buildings located in high seismic regions.

## 4.1 PROPOSED PROCEDURE FOR ACHIEVING PREFERRED SEISMIC PERFORMANCE IN HOSPITAL BUILDINGS

The preferred seismic performance objective of hospital buildings is to remain *Occupiable* after an earthquake. This requires the building to have *only* incurred *no* or *limited* structural damage. For the purpose, *yielding* of longitudinal reinforcement in tension in structural members indicating a transition from state of *no structural damage* to *limited structural damage* in the structure can be considered to be the limit state. Thus, to meet the above performance objective, current study proposes a drift demand ($\delta_y$) at onset of yielding of longitudinal steel in structural element to be imposed only after the meeting an *allowable* displacement demand ($\delta_{allowable}$) in the building (Figure 4.1). Traditionally, approximate estimate of displacement or drift demands imposed on typical buildings are evaluated using two criteria, namely (a) *equal displacement criteria* for long-period structures with fundamental period greater than 0.6 seconds, and (b) *equal energy criteria* for short-period structures with fundamental period less than 0.5 seconds [Riddell, *et al.*, 1989; Newmark and Hall, 1973]. The above are presented schematically in Figure 4.2. For equal displacement criteria, $\delta_{allowable}$ is $\delta_e$ (Figure 4.2 (a)), and $\delta_{eqe}$ for equal energy criteria (Figure 4.2 (b)). Steps to estimate $\delta_e$ using equal displacement criteria are (Figure 4.2 (a)):

(1) Determine elastic lateral force ($H_e$) as:

$$H_e = \left[\frac{ZI}{2}\left(\frac{S_a}{g}\right)\right] W \tag{4.1}$$

(2) Determine design base shear ($H_d$) as:

$$H_d = \frac{H_e}{R} \tag{4.2}$$

(3) Perform seismic design as per relevant Indian Standards and check adequacy based on nonlinear static response assessment of the study building;

(4) Redesign inadequate members;

(5) Obtain nonlinear static response curve of study building;

(6) Identify design drift $\delta_d$ corresponding to $H_d$ from nonlinear static response curve;

(7) Obtain elastic drift $\delta_e$ corresponding to $H_e$ using similar triangles.

Steps to estimate $\delta_{eqe}$ using equal displacement criteria are (Figure 4.2 (b)):

(1) Repeat steps (1) to (6) above;

(2) Compute area of triangle OA$\delta_e$;

(3) Obtain $\delta_{eqe}$ by iteration, until area of triangle OA$\delta_e$ and area OH$_{max}$B$\delta_{eqe}$ are equal.

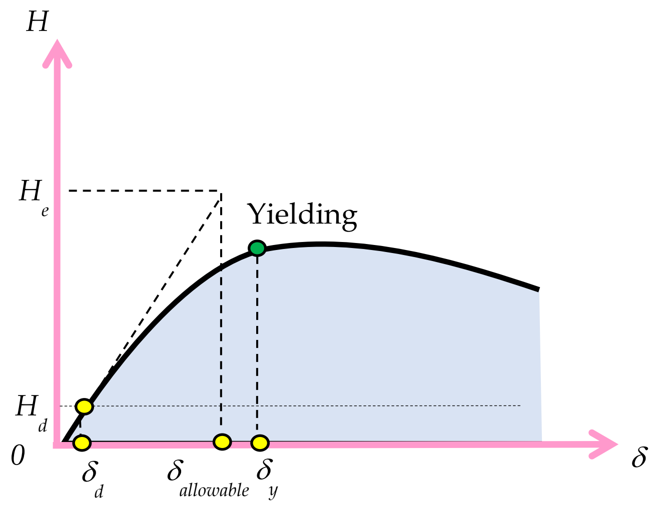


**Figure 4.1**: Proposed Performance Criteria

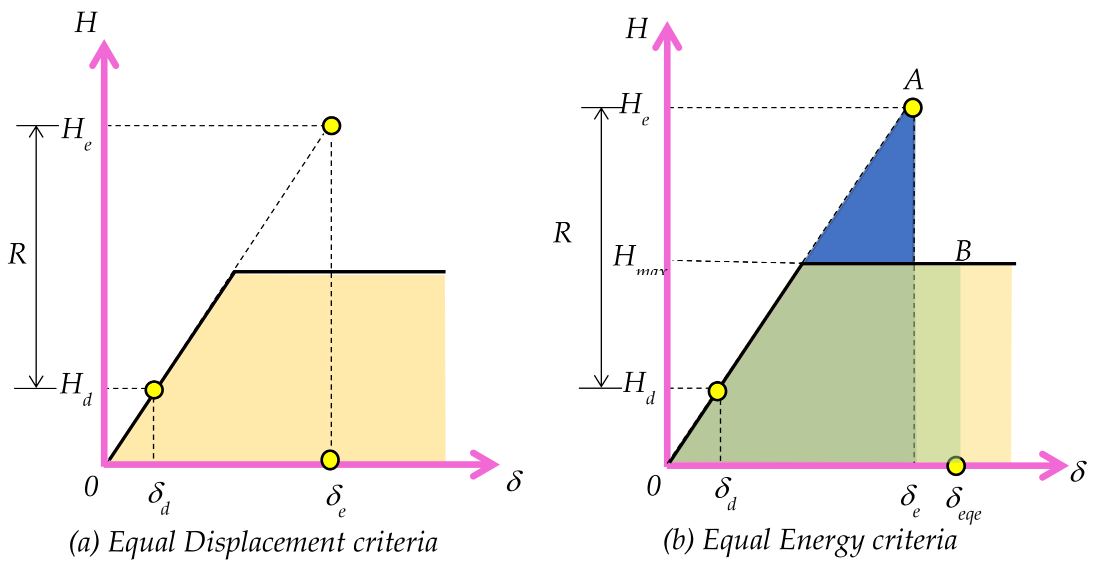


**Figure 4.2**: Estimation of approximate displacement demands

## 4.2 SELECT INELASTICITY IN STUDY BUILDINGS

M25 grade concrete for beams and M30 for columns and structural walls are used in study buildings (Section 4.3). Concrete confinement model recommended by Mander (Section 2.5) is followed and the nonlinear concrete stress-strain curve idealized for use as input in PERFORM3D. For the idealization, Mander stress-strain curve until a drop in 20% strength is considered. Fe500 grade reinforcement is used to develop stress-strain curve in two parts. (Figure 4.3). They are: (a) linear elastic part up to the characteristic yield stress $f_y$ and strain 0.002+($f_y$/$E_s$), and (b) linear plastic part up to $f_y$ and strain 0.12 [Sunitha, 2017; Deshmukh, 2017]. Further, lumped inelasticity in ends of beams for a length of 0.5*D* (to facilitate better interaction between structural walls and connected beams) (Section 2.4.1), fiber inelasticity is defined in columns and structural walls; in columns, fibres are defined for a length of 0.5*D* and across the height in structural walls [Section 2.4.2.1] (Figure 2.11).

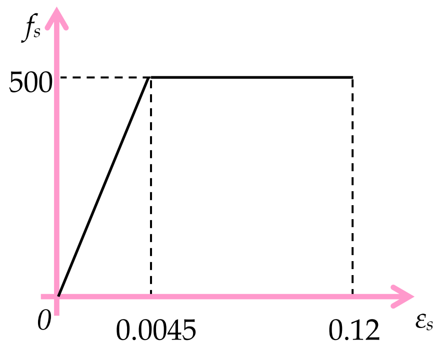


**Figure 4.3**: Stress-strain relation of reinforcement used in the study

## 4.3 FUNDAMENTAL DYNAMIC PROPERTIES and LATERAL FORCE DEMAND ON STUDY BUILDINGS

Details of study buildings are discussed in Chapter 3 (Section 3.5). In all, 7 study buildings are considered; Building A (original building), Building B (structural configuration of Building A revised to preclude torsional first mode), Building C (structural design of Building B revised to comply with IS1893 (1), and IS13920 (2016) provisions), Building D (structural system of Building C modified to include structural walls forming 1% SPD), Building E (structural system of Building C modified to include structural walls forming 2% SPD), Building F (structural system of Building C modified to include structural walls forming 3% SPD, and Building G (structural system of Building C modified to include structural walls forming 4% SPD). Based on the given dimensions, numerical model of Building A is first developed, and fundamental mode shape investigated. It was observed that Building A has torsional fundamental mode with less mass participation. In general, corner rectangular columns in the diagonal direction are overstressed in this mode of oscillation. This is because, least lateral (bending and shear) resistance is offered by rectangular (or square) columns about an axis not parallel to their sides. Such detrimental behaviour will result in severe damages especially in columns in Building A. Thus, as a corrective action, an attempt to push the fundamental torsional mode to higher modes was made by revising the orientation of given columns to get Building B. In spite of achieving the preferred mode shape in Building B, poor Nonlinear Time History Analysis (NTHA) results and seismic behaviour was observed with severe damages in columns. In addition, Buildings A and B were not complying with IS 13920 clauses for member sizes and CBSR. Therefore, as the next corrective action, Building B was redesigned to comply with IS13920 to get Building C. Though improved seismic behaviour could be attained in Building C under NTHA, preferred performance objective as per equal displacement criteria (based on the fundamental period) could not be met. Hence, *moment frame* buildings A, B, and C is concluded to be a poor structural system for hospital buildings in high seismic regions. Further, to be in line with the recommendations given for structural systems for hospital buildings, buildings D, E, F, and G considered are wall-frame systems with variations in SPDs of structural walls in Building C [NDMA, 2016].

Fundamental dynamic properties of Buildings A—G are listed in Table 4.1 (Figure 4.4). In general, the fundamental period of buildings A—G increased with increasing stiffness due to change in design, structural system and pertaining SPDs. Alongside, a reduction in effective mass is also observed in buildings B—G due to possible transition from shear mode shape in moment frames (buildings B—C) to a more flexure predominant mode shape in wall-frame buildings D— G. Further, this reduction is almost negligible between buildings with a particular structural system. And, due to poor configuration and proportioning, Building A has the least effective mass.

**Table 4.1**: Fundamental dynamic properties of study buildings

| *Building* | *Structural System* | *Fundamental Period (Seconds)* | *Effective mass factor* | *Mode Shape* |
|---|---|---|---|---|
| A | OMRF | 1.06 | 0.53 | Torsional |
| B | OMRF | 1.07 | 0.82 | Translational |
| C | SMRF | 0.95 | 0.82 | Translational |
| D | | 0.51 | 0.73 | Translational |
| E | Wall - Frame | 0.47 | 0.71 | Translational |
| F | | 0.36 | 0.69 | Translational |
| G | | 0.33 | 0.70 | Translational |

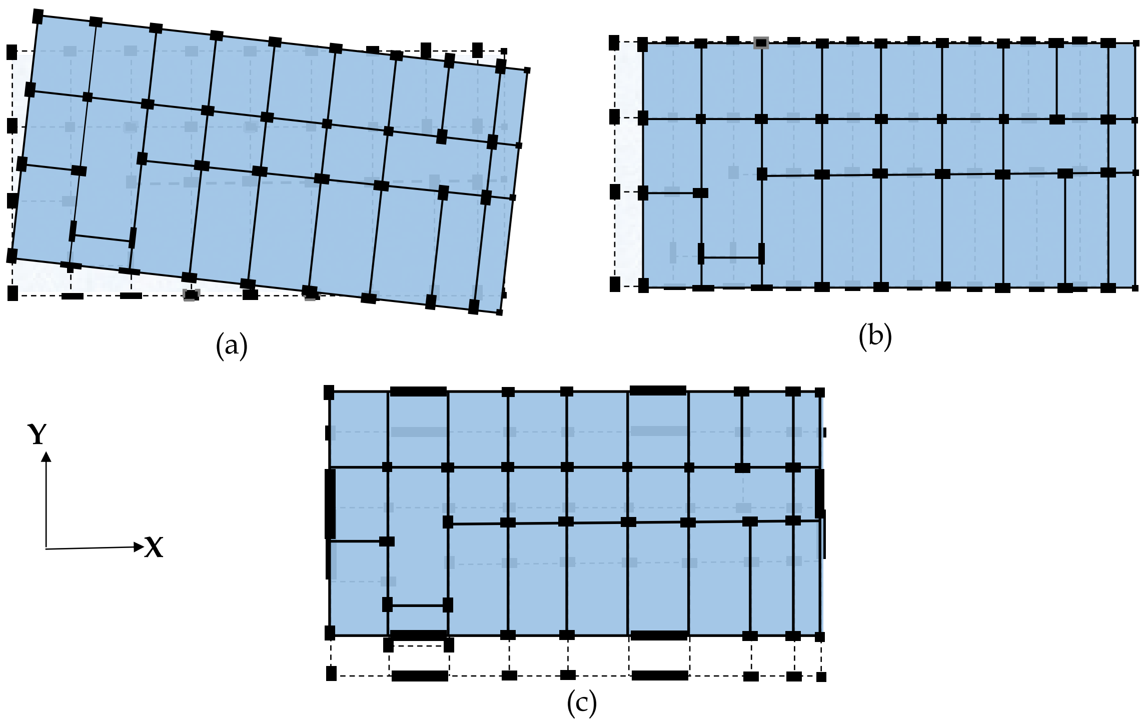


**Figure 4.4**: Plan-view of fundamental mode shapes of buildings: (a) A, (b) B, and (c) D

## 4.4 INELASTIC RESPONSE OF STUDY BUILDINGS

Inelastic response of study buildings is investigated using nonlinear static and nonlinear time history analyses results. These analyses predict displacement demands imposed on the buildings. Firstly, the maximum displacement demands imposed during NSA and NTHA are compared to check non-exceedance of these demands during NTHA. This is because NTHA provides more realistic estimates of seismic demands compared to NSA, but NSA is reasonably easy to perform in design practice. Thus, if demands imposed during NSA is higher than those imposed during NTHA, it is appropriate to assume seismic safety of the structure. Secondly, to comply with the proposed procedure to obtain preferred seismic performance in hospital buildings (Section 4.1), $\delta_y$ is also monitored during NSA and NTHA in Buildings B—G. Details of investigations are given hereunder.

### 4.4.1 Nonlinear Static Response

Displacement-controlled NSA is performed of Buildings B—G, and structural damage limit states are monitored (Section 3.2). NSA of Building A is not carried out due to low mass participation in fundamental mode (Table 4.1) [FEMA 356, 2000].

#### *4.4.1.1 Observations from monitored limit states of structural damage*

In Building B, intermediate columns also incurred damage, but most beams remained elastic (Figure 4.5 (a)). This is because of low CBSR. In Building C, while intermediate columns remained elastic, severe damage incurred in most beams, and few column bases incurred damage (Figure 4.5 (b)). This is due to the revised design of structural elements as per IS13920, alongside adequate $\beta$. In Building D, longitudinal reinforcement in structural walls yielded before ends of beams (Figure 4.5 (c)). This can be attributed to higher seismic demands imposed on structural walls due to increase in stiffness. Also, most beams and one structural wall reached crushing limit state, and all structural walls yielded. In buildings E and F, most beams yielded but reduction in yielding in structural walls and crushing in beams were observed. Similarly, in Building G, most beams yielded and only few beams reached crushing limit state. This is due to increase in stiffness in these buildings with higher wall SPD and in turn improved lateral resistance (Figure 4.6 (a) and (b)). Nonlinear static response curves of Buildings B—G are normalized; base shear is normalized with maximum base shear capacity and drift with maximum drift capacity (Section 3.4.2 (b)) and presented (Figure 4.7).

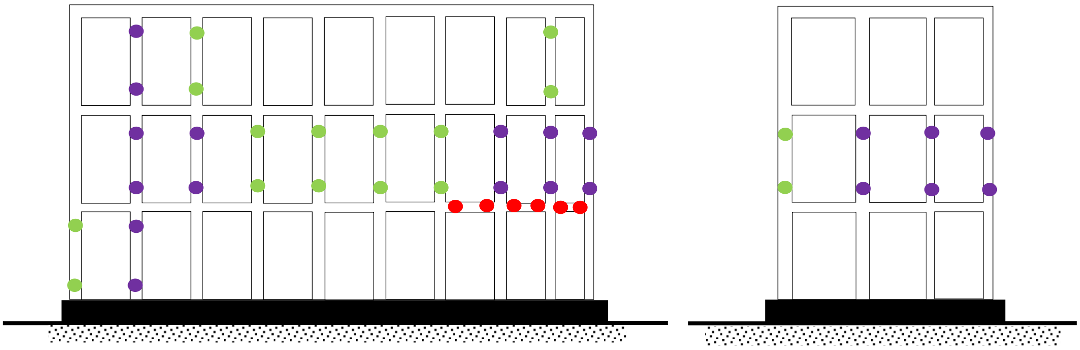

(a)

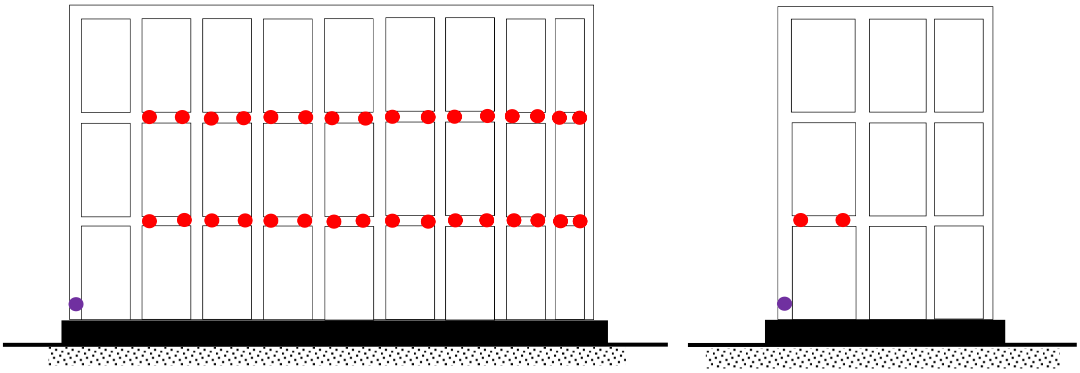

(b)

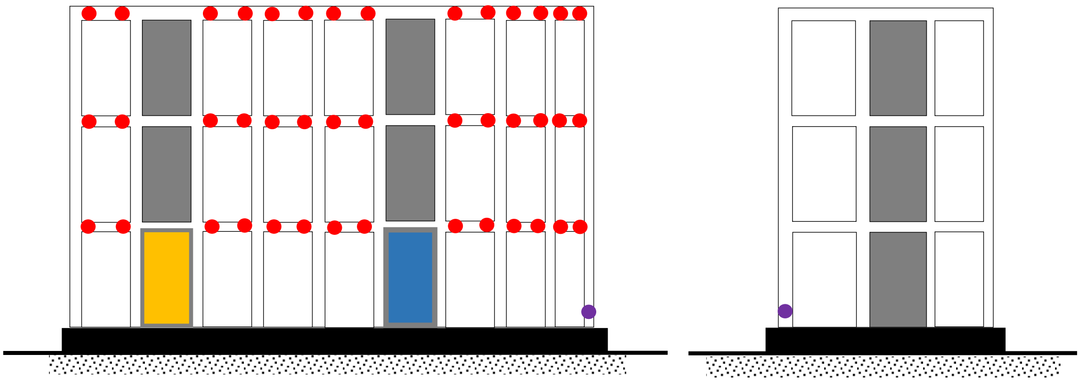

(c)

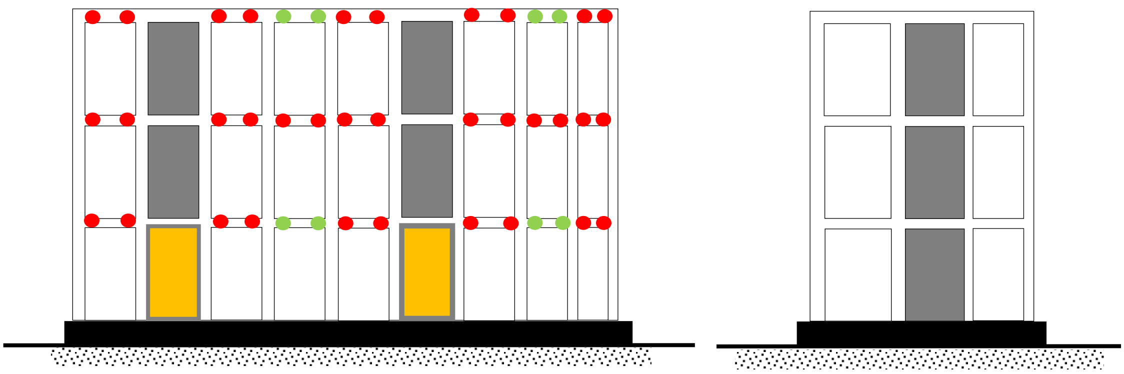

(d)

**Figure 4.5**: Structural Damages in study buildings: (a) B, (b) C, (c) D, and (d) E

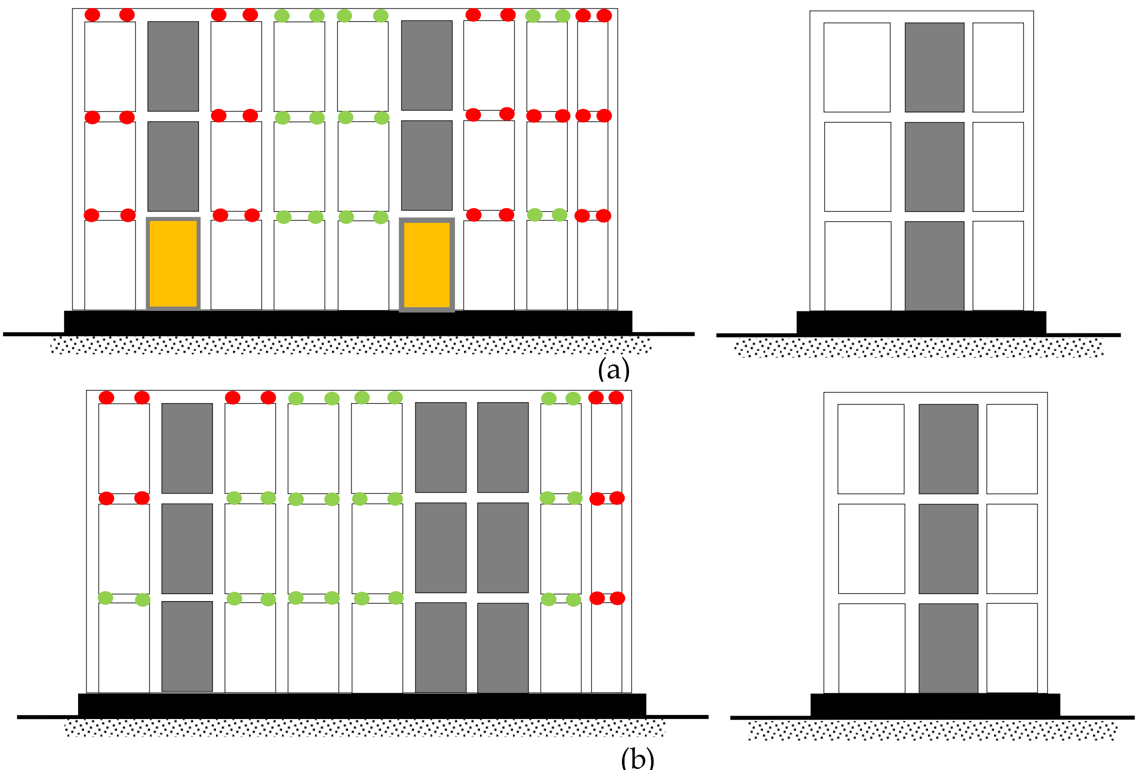


- Yielding of longitudinal reinforcement in beams or columns
- Yielding of longitudinal reinforcement in structural walls
- Crushing of confined concrete in beams
- Spalling of unconfined concrete in structural walls
- Crushing of confined concrete in columns

**Figure 4.6**: Structural Damages in study buildings: (a) F, (b) G

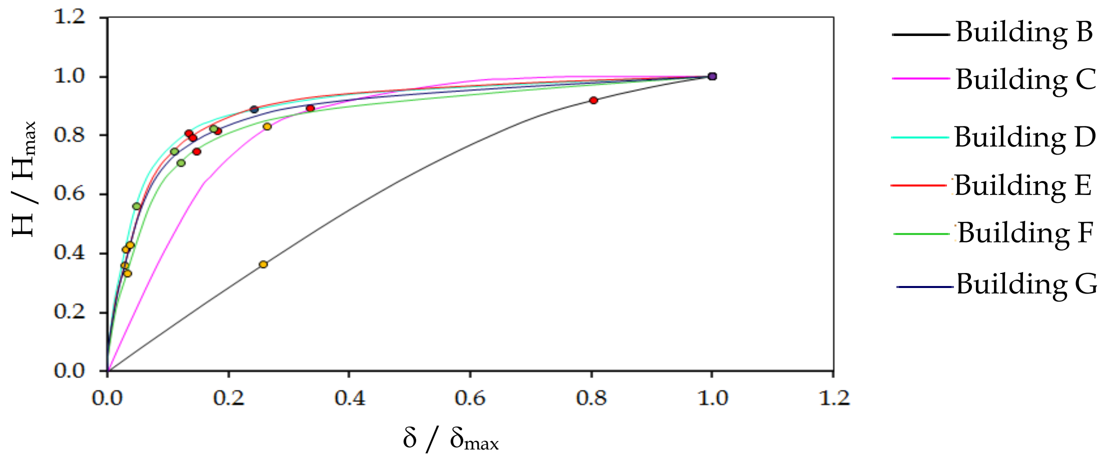


- Yielding of longitudinal reinforcement in beams or columns
- Yielding of longitudinal reinforcement in structural walls
- Crushing of confined concrete in beams
- Spalling of unconfined concrete in structural walls
- Crushing of confined concrete in columns

**Figure 4.7**: Normalized static response curves and limit states of structural damage

#### *4.4.1.2 Estimation of earthquake resistant virtues of study buildings*

In general, the earthquake resistant virtues (EQR) of buildings are good structural configuration, minimum lateral stiffness, lateral strength, and lateral ductility. Deformability which is the maximum drift capacity and ductile collapse mechanism are also be considered as good EQR virtues (Figure 4.8). Here the lateral stiffness, strength, ductility, and deformability are estimated from idealized nonlinear static response curves of study buildings [Figure 4.8].

##### *(a) Lateral stiffness, ductility, and deformability*

Lateral stiffness, ductility, and deformability of study buildings are tabulated in Table 4.2. In general, lateral stiffness increased with increase in column sizes (Building B to Building C) and SPD of structural walls (Buildings D-G). Lateral Ductility of Building C is more than that of Building B due to early onset of yielding in stiffer Building C. But, ductility reduced with increase in SPD of structural walls (Buildings D – G). This may be due to incurring of less damage in these buildings with increase in strength with increase in stiffness. Further, deformability reduced with increase in stiffness and strength.

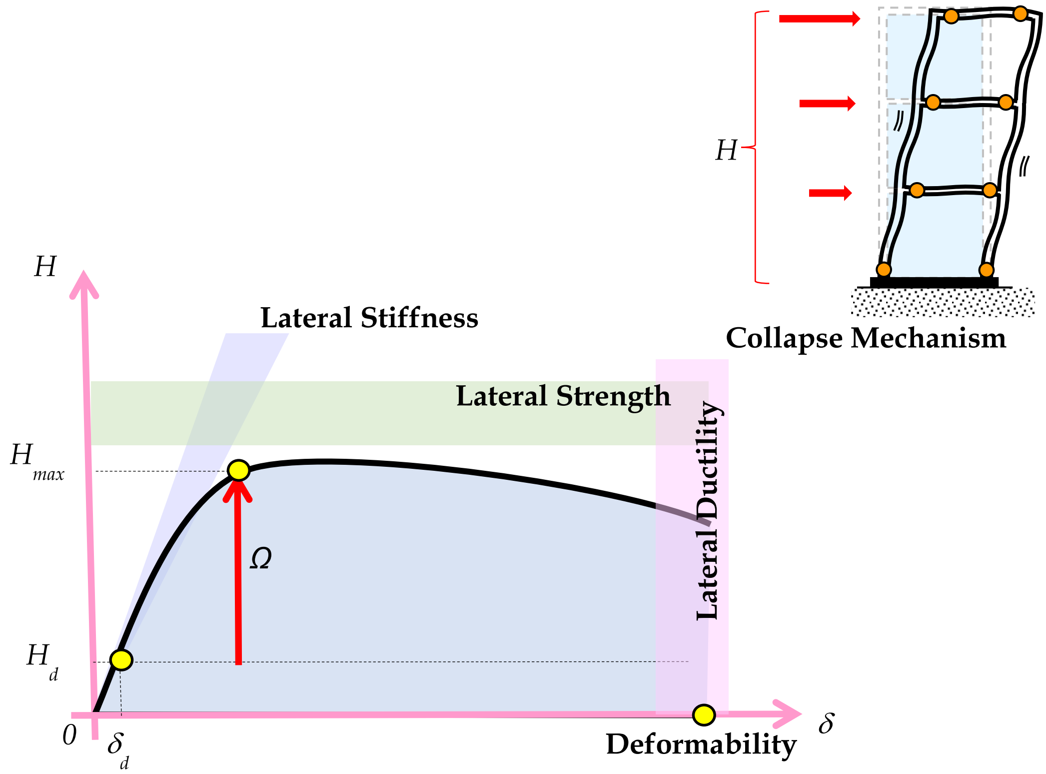


**Figure 4.8:** Virtues of Earthquake Resistant Structure

**Table 4.2**: EQR Virtues of Study Buildings

| Building | EQR Virtues | | |
|---|---|---|---|
| | Stiffness (kN/m) | Ductility | Deformability (%) |
| **B** | 68675 | 2.42 | 1.8 |
| **C** | 87997 | 5.89 | 4.0 |
| **D** | 401083 | 14.00 | 3.8 |
| **E** | 618215 | 11.68 | 3.2 |
| **F** | 686123 | 10.43 | 3.0 |
| **G** | 1385892 | 9.94 | 2.5 |

***(b) Lateral Strength***

Here, lateral strength is represented by Overstrength (Ω), the ratio of maximum lateral strength and design lateral strength (Figure 4.9). It is observed that overstrength increased with increase in SPD of structural walls. But, moment frame Building B has low stiffness and strength compared to wall-frame buildings, analogous to buildings in low seismic regions where gravity load dominates lateral loads, and hence higher overstrength [Navin, and Jain, 1995].

### 4.4.2 Nonlinear Time History Response

Ground motion details selected for NTHA are tabulated in Table 4.3 [Sunitha *et al.*, 2017; Mittal *et al.*, 2012]; 28 ground motion records in total are used to obtain randomness in the seismic behaviour. Acceleration response spectra of all 28 ground motions is presented in Figure 4.10. Spectral amplitude scaling is adopted for scaling ground motions in this study where spectral value of the ground motion is scaled at the elastic natural period to match the design spectral value (Section 2.3.1) (Figure 3.11).

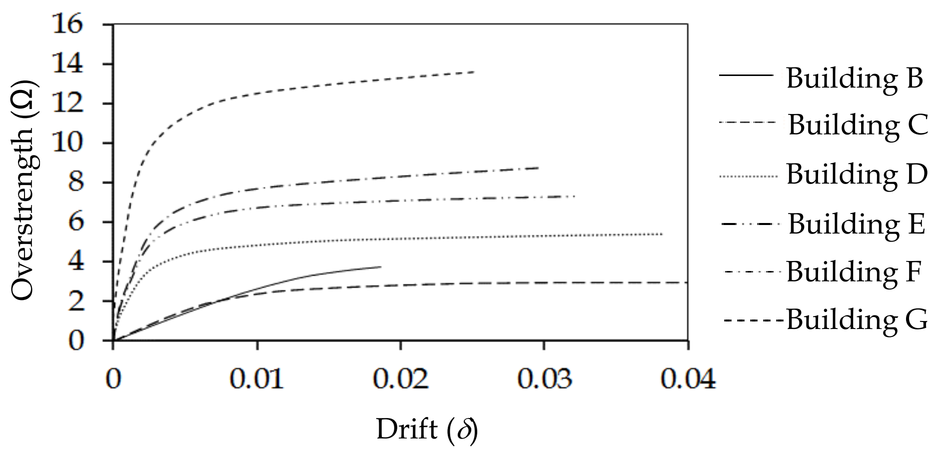


**Figure 4.9**: Overstrength(Ω) in study buildings

**Table 4.3**: Characteristics of ground motions used for NTHA

| No. | Event | Station | Year | $M_w$ | Duration (Seconds) | Predominant Frequency (Hz) | PGA (g) | Epicentral distance(km) |
|---|---|---|---|---|---|---|---|---|
| 1 | Kern County | Taft | 1952 | 7.36 | 21.00 | 1.367 | 0.159 | 36.89 |
| 2 | Tabas | Dayhook | 1978 | 7.35 | 21.00 | 2.563 | 0.324 | 13.94 |
| 3 | San Fernando | Palmdale Fire Station | 1971 | 6.60 | 30.00 | 1.147 | 0.133 | 25.4 |
| 4 | Chi Chi | TCU 047 | 1999 | 7.62 | 90.00 | 0.817 | 0.298 | 35.0 |
| 5 | Imperial Valley | Plaster City | 1979 | 6.50 | 19.00 | 2.637 | 0.042 | 31.7 |
| 6 | | Niland Fire Station | | | 40.00 | 0.977 | 0.069 | 35.9 |
| 7 | | Delta | | | 98.20 | 0.598 | 0.351 | 43.6 |
| 8 | | Coachella Canal #4 | | | 28.60 | 1.880 | 0.115 | 49.3 |
| 9 | Park Field | Cholame 3W | 1983 | 6.40 | 40.00 | 98.56 | 0.078 | 30.4 |
| 10 | | Gold Hill 3E | | | 39.99 | 0.781 | 0.094 | 29.2 |
| 11 | | Fault Zone 3 | | | 39.99 | 1.538 | 0.139 | 36.4 |
| 12 | | Fault Zone 10 | | | 39.99 | 0.708 | 0.073 | 30.4 |
| 13 | Superstition Hills | Wildlife Lique. Array | 1987 | 6.30 | 29.80 | 2.319 | 0.207 | 24.7 |
| 14 | Loma Prieta | Hollister-South Pine | 1989 | 6.90 | 59.95 | 1.025 | 0.371 | 28.8 |
| 15 | | Red Wood City | | | 200.00 | 0.903 | 0.273 | 47.9 |
| 16 | | Salinas | | | 39.95 | 1.416 | 0.091 | 32.6 |
| 17 | Cape Mendocino | Eureka-Myrtle and West | 1992 | 7.10 | 44.00 | 0.549 | 0.154 | 44.6 |
| 18 | | Fortuna Boulevard | | | 44.00 | 0.342 | 0.116 | 23.6 |
| 19 | Landers | Fire Station | 1992 | 7.30 | 43.20 | 0.708 | 0.152 | 24.9 |
| 20 | | Palm Springs Airport | | | 59.00 | 1.025 | 0.076 | 37.5 |
| 21 | | Desert Hot Spring | | | 49.20 | 2.124 | 0.171 | 23.2 |
| 22 | Northridge | Lake Hughes #1 | 1994 | 6.70 | 31.98 | 1.245 | 0.087 | 36.3 |
| 23 | | Downey-Co Maint. Bldg. | | | 20.00 | 5.029 | 0.230 | 47.6 |
| 24 | | LA 116$^{th}$ Street School | | | 39.98 | 2.271 | 0.1333 | 41.9 |
| 25 | Kobe | Nishi-Akashi | 1995 | 6.90 | 40.30 | 2.075 | 0.483 | 7.08 |
| 26 | | Kakogawa | | | 40.30 | 2.734 | 0.251 | 22.5 |
| 27 | | Morigawachi | | | 198.00 | 0.894 | 0.214 | 24.8 |
| 28 | Hector Mine | Hector | 1999 | 7.13 | 46.00 | 0.793 | 0.265 | 11.6 |

#### *4.4.2.1 Observations from monitored limit states of structural damage*

In Building B, most intermediate columns reached their crushing limit state under most ground motions, thereby forming an undesirable collapse mechanism. In particular, under 4 ground motions, beams did not incur any damage, while damages occurred in few columns under two ground motions. In Building C, no column damage is observed under any ground motions, but beams reached crushing limit state under ten ground motions. In Building D, yielding of reinforcement in beams, columns and structural walls is observed under most ground motions. Also, under 2 ground motions, structural walls reached crushing limit state. Reduction in extent of damages were observed with increase in SPD of structural walls in buildings. In Building E and F no yielding occurred under about nine ground motions, but yielding occurred only under 3 ground motions in Building G. Further, no structural elements reached crushing limit state under any ground motions in buildings E, F, and G (Figure 4.11).

### 4.5 COMPARISON OF LATERAL DEFORMATION BEHAVIOUR

Drift responses from nonlinear static and time history analysis are compared to confirm the seismic bahaviour of study buildings. Firstly, *maximum* drift demands imposed during NTHA ($\delta_{NTHA}$) are confirmed to not exceed demand imposed during NSA ($\delta_{NSA}$) (Figure 4.12). If $\delta_{NTHA}$ is less than $\delta_{NSA}$, drift demands estimated from NSA are assumed to be a reasonable demand imposed on study buildings. For the purpose, drift ratio ($\delta_{NTHA}$ / $\delta_{NSA}$) is estimated of study buildings.

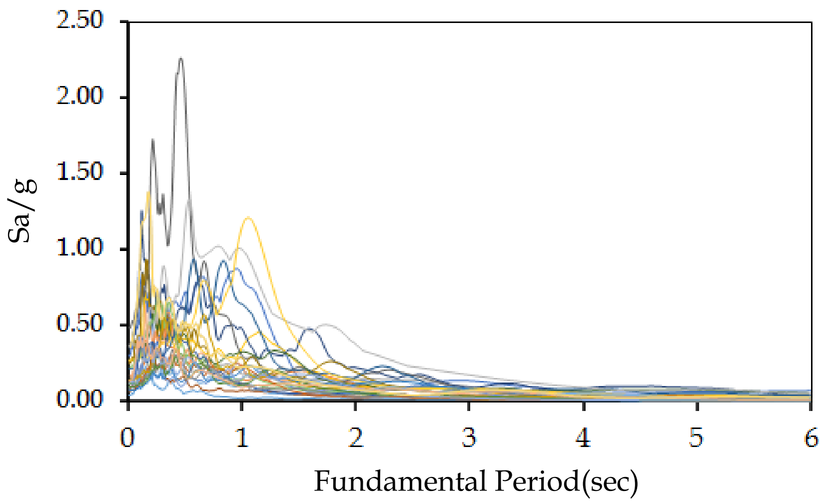


**Figure 4.10**: Acceleration response spectrum for study buildings

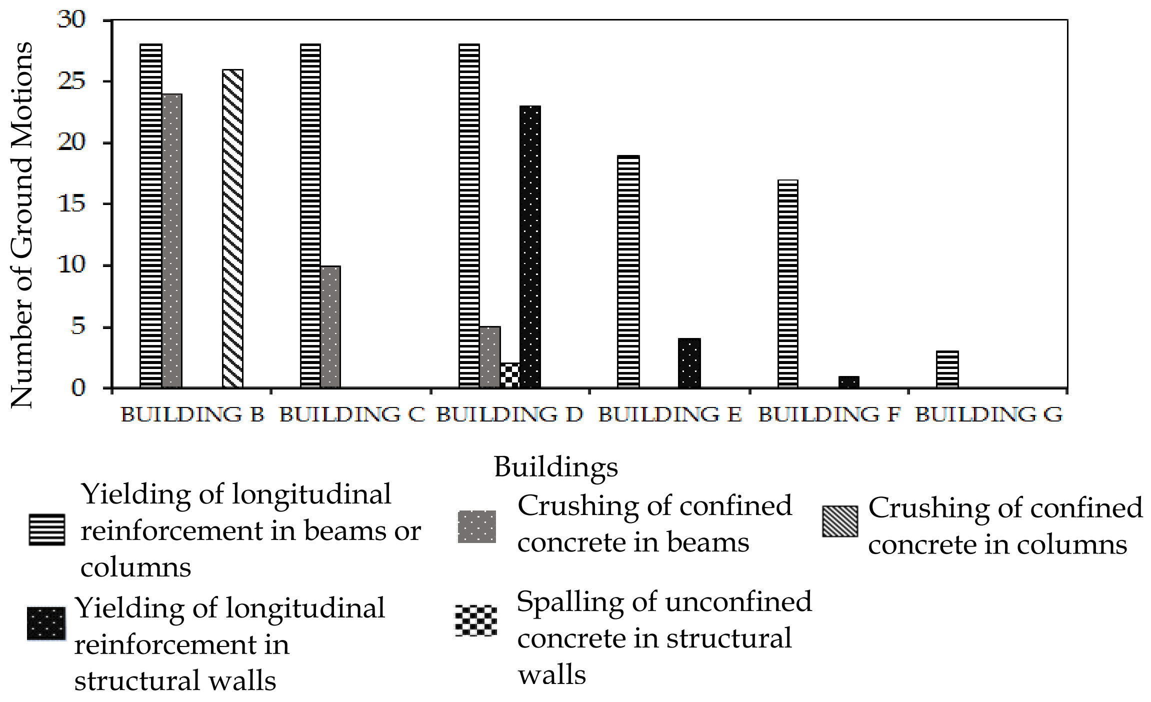


**Figure 4.11**: Limit states of structural damage reached during NTHA

Here, $\delta_{NTHA}$ is obtained under considered ground motions and $\delta_{NSA}$ is a single value obtained for each study building from NSA (Figure 4.18). It is observed that in Building B $\delta_{NTHA}$ exceeds $\delta_{NSA}$ under few ground motions, and in Building C the demands are almost acceptable. Further, due to the stiffness increase in the structural plan of study buildings, overall drift reduces with the increase in SPD of structural walls.

Secondly, *yield* drift demands corresponding to limit state of yielding in structural members imposed during NTHA $\delta_{yield}$ (corresponding to $\delta_y$ in Figure 4.1) are checked against $\delta_{allowable}$ (corresponding to $\delta_{allowable}$ in Figure 4.2) demand imposed during NSA. This is to ensure the preferred *Occupiability* seismic performance of study buildings as proposed in Section 4.1 (Figure 4.13). If $\delta_{allowable}$ is less than $\delta_{yield}$, occupiability performance is assumed to be achieved in study buildings. Here, $\delta_{allowable}$ is a single value obtained for each study building from NSA. It is observed that in building B, C, D, E and F, $\delta_{allowable}$ exceeds $\delta_{yield}$ under most ground motions, and in Building G $\delta_{yield}$ exceeds $\delta_{allowable}$ under 2 ground motions almost acceptable. Thus, Building G is observed to provide the preferred occupiability performance under actual ground motions also.

Performance criteria evaluated as per the proposed procedure confirms *Occupiability* performance of Building G. Also, extent of damages in Buildings D—F at $\delta_{allowable}$ and percentage difference between $\delta_{allowable}$ and $\delta_y$, are reducing as the wall plan density is increasing; difference between $\delta_{allowable}$ and $\delta_y$ in buildings D—F are 50%, 35% and 25%, respectively. This can be attributed to increased strength and stiffness of the structure. Further, structural damages in buildings D—F at $\delta_y$ and $\delta_{y,idealised}$ (idealized yield drift obtained from nonlinear static response curve) are investigated (Figure 4.14 and 4.15). This is crucial as past literature reports during 1994 Northridge and 2015 Nepal earthquake, the Granada Hills Community Hospital, and TshoRolpa Hospital suffered less structural damage but was still declared structurally unsafe to occupy. Thus, the structure accruing less damage at $\delta_{allowable}$ is also critical and hence investigated for recommending corrective design actions for preferred performance. $\delta_{y,idealised}$ is identified for monitoring to check if a lesser conservative drift value higher than first yield can be recommended in the proposed procedure as the drift limit for meeting the preferred performance.

In Building D, most of the structural walls and beams yielded before reaching $\delta_{allowable}$ and $\delta_{y,idealised}$, *i.e.*, 8% of beams and 66% of total structural wall—no of (beams, structural walls or columns) members yielded/total number of members (beams, structural walls or columns), accrued damages under all ground motions and during NSA (Table 4.4).

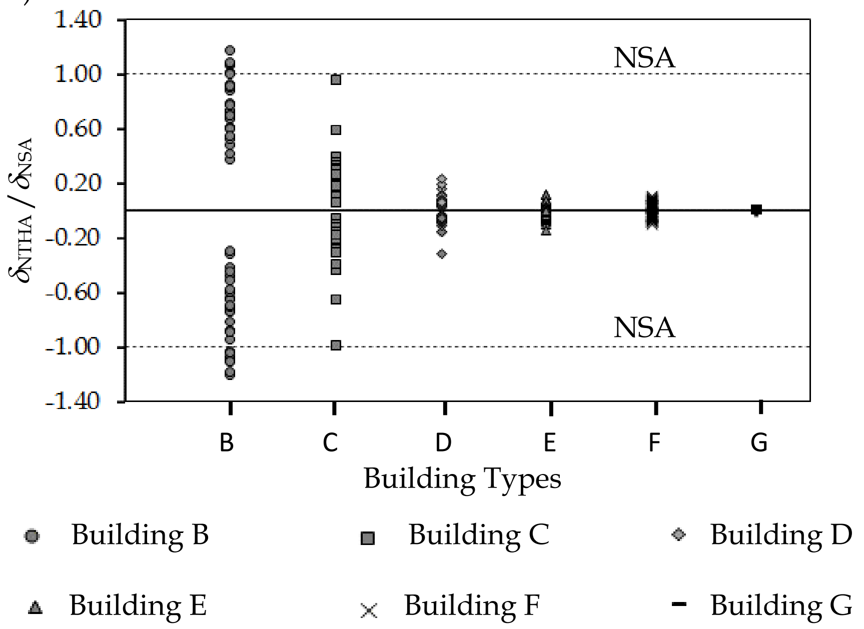


**Figure 4.12**: Maximum drift ratio in study buildings

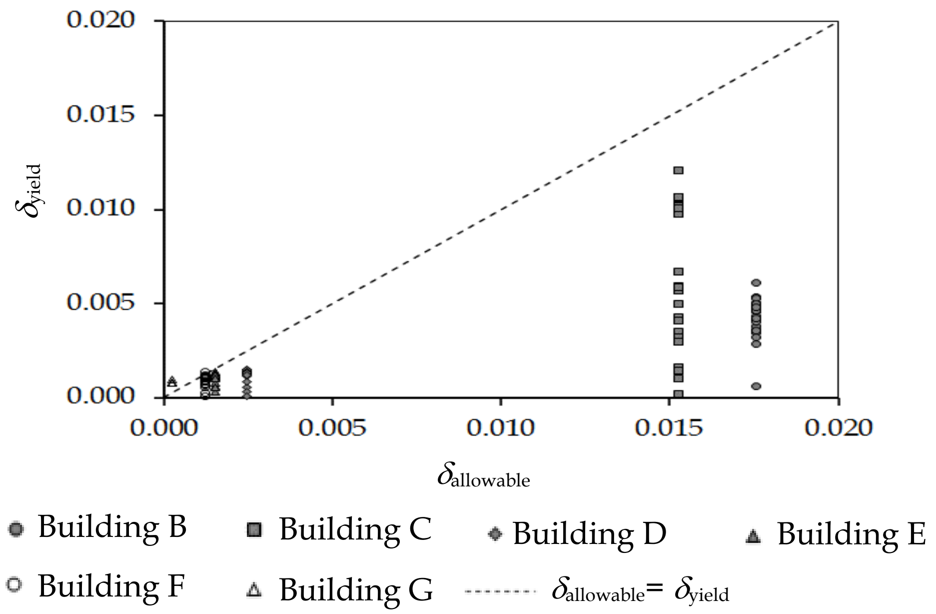


**Figure 4.13**: Confirming *Occupiability* performance in study buildings

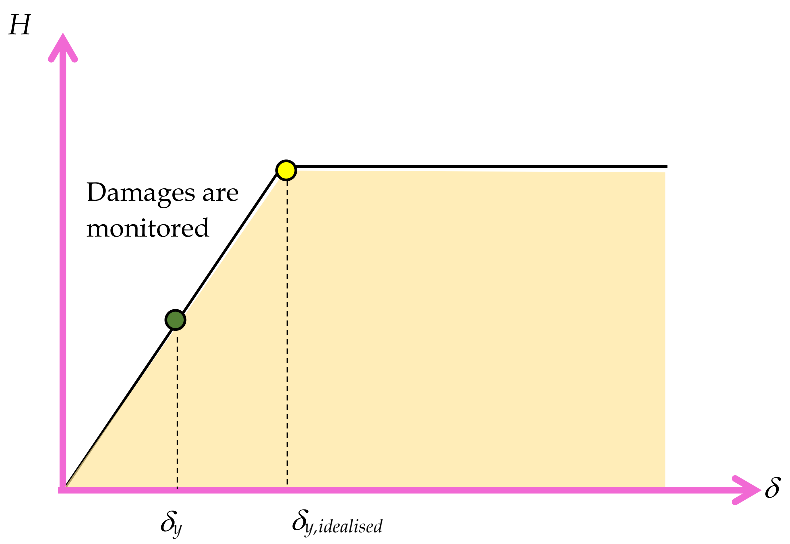


**Figure 4.14**: Schematic of drift values at first yield ($\delta_y$) and idealized yield ($\delta_{y,idealised}$)

Percentage reported from NTHA is the average value obtained under 28 ground motions, and the outliers are reported separately. In Building E, damages in structural walls decreased under most ground motions before reaching $\delta_{allowable}$, damages in beams are similar to that in Building D, but structural walls incurred damages before reaching $\delta_{y,idealized}$ *i.e.*, 10% of beams and 12.5%. In case of Redwood city and Park Field

Fault Zone 3 ground motions, damages in structural walls were found to be 62.5%. Thus, Buildings D and E cannot be recommended for hospital use as they fail to provide the occupiability performance, post-earthquake. In Building F, no damages were observed in structural walls before $\delta_{allowable}$ and $\delta_{y,idealized}$ is reached, *i.e.*, only 6% of beams yielded under all ground motions and during NSA. Hence, in Building F, though the criteria for preferred performance as per the proposed procedure is not satisfied, only a few beams are incurring damages. Thus, the drift criteria proposed in this study to meet *Occupiability* performance in hospital buildings is observed to be stringent. Also, even at $\delta_{y,idealized}$, since damages have not progressed in Building F, Building F can also be recommended for use, post-earthquake. Thus, wall-frame building with 3% wall SPD is also observed to provide occupiability performance from this study. Finally, in Buildings D—G, column bases did not incur any damage.

## 4.6 COLUMN TO BEAM STRENGTH RATIO (CBSR (β))

There are no explicit recommendations for hospital buildings except the value 2 for CBSR values in NDMA document. Thus, the CBSR values in buildings D, E, F, and G are evaluated to recommend the desirable range in these wall-frames buildings (Table 4.5). A desirable collapse mechanism is formed for all buildings with wall-frame structural systems, i.e., beams accrue damages first, in structural walls, second, and in columns.

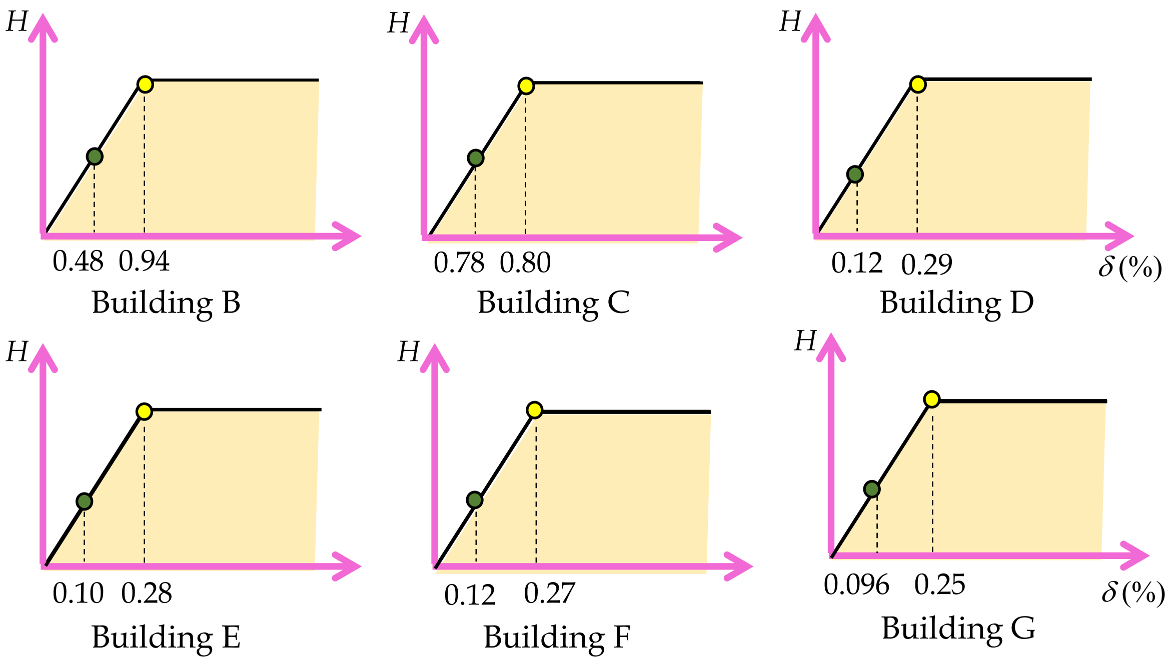


**Figure 4.15**: Salient drift values at first yield ($\delta_y$) and idealized yield ($\delta_{y,idealised}$)

**Table 4.4**: Quantification of Structural damages in wall-frame study buildings

| Building | Analysis | Percentage of structural members damaged at salient drifts | | | | | |
|---|---|---|---|---|---|---|---|
| | | $\delta_y$ | | $\delta_{allowable}$ | | $\delta_{y,idealised}$ | |
| | | Beam | SW | Beam | SW | Beam | SW |
| D | NSA | 1.5 | - | 6 | 66 | 8 | 66 |
| | NTHA | 2.5 | - | 7 | 66 | 7 | 66 |
| E | NSA | 1.5 | - | 7 | - | 10 | 12.5 |
| | NTHA | 2.5 | - | 5 | 12.5 | 12 | 12.5 |
| F | NSA | 3.5 | - | 6 | - | 9 | - |
| | NTHA | 1.5 | - | 5 | - | 9 | - |

**Table 4.5**: CBSR values of wall-frame buildings

| Building | CBSR Value |
|---|---|
| **D, E, F, G** | 2.0-2.5 |

Hence CBSR required is between 2—2.5 in these buildings to meet the occupiability performance objective.

## 4.7 CONCLUSIONS

Salient conclusions from the work carried out as part of this Chapter are:

(a) SMRFs designed and detailed as per IS456:2000, IS1893 (1) and IS 13920 (2016) do not meet the *Occupiability* performance objective post-earthquake, as proposed in this study. Wall-frame structural systems should be adopted to ensure the preferred performance;

(b) Wall-frame structural systems designed and detailed as per IS456:2000, IS1893 (1) and IS 13920 (2016) with SPD 3%—4%, and CBSR 2.0—2.5 are recommended for hospital buildings in high seismic regions to meet occupiability performance objective post-earthquake; and

(c) It is required to meet at least $\delta_{y,idealised}$ before $\delta_{allowable}$ (the approximate drift demand imposed in typical wall-frame buildings considered in the study) to achieve *Occupiable* performance in hospital buildings, post-earthquake.

…

*Blank Page*

# 5

# Summary and Conclusions

## 5.0 OVERVIEW

Design codes do not mandate a suitable structural system to meet the preferred seismic performance for *hospital* buildings, but prescriptive design guidelines are recommended by NDMA. Severe damages to hospital buildings have been observed in past earthquakes, thereby necessitating reliable understanding of earthquake behavior of these buildings. This will help *fine-tune* the available design guidelines. Based on linear and nonlinear static and dynamic analyses studies, present study investigates the seismic performance of *wall-frame* hospital buildings to quantitatively verify the design guidelines that help meet desire *Occupiability* seismic performance.

## 5.1 SUMMARY

The following is a summary of the work carried out as part of this thesis:

(1) For understanding seismic behaviour of *wall-frames*, pilot linear and nonlinear behaviour studies of 2D wall-frames for varying plan aspect ratio, are carried out;

(2) To quantify the structural damages incurred, strain limit states of structural damages in select members defined with inelastic fibers are identified and monitored, during nonlinear static and dynamic analyses;

(3) To propose *Occupiability* of wall-frame hospital buildings later, salient drifts at *design* lateral force, *elastic maximum* drift and *allowable* drifts, are obtained and investigated;

(4) For realistic understanding of seismic behaviour of wall-frame hospital *buildings*, linear and nonlinear behaviour studies of 3D wall-frames with plan aspect ratio more than 4 (confirmed from pilot studies) for varying SPDs, are carried out. Further, strain limit states of structural damages as explained in (b) above are used;

(5) To achieve preferred *Occupiability* seismic performance in hospital buildings, a method agreeing with a traditional approach is proposed, to estimate the displacement demand imposed on study hospital building;
(6) To confirm reasonably good linear (fundamental period, effective mass factor and mode shapes) and nonlinear behaviour (damages incurred at identified strain limit states) are examined of all study buildings. Further, the proposed procedure in (e) above is used to examine *Occupiability* seismic performance. In addition, structural damages at salient drifts corresponding to *first yield*, *idealized yield* and *allowable drift* are also quantified; and
(7) Finally, to achieve the *Occupiability* seismic performance, appropriate structural system requirements, namely seismic structural configuration, Structural Plan Density (SPD) of structural walls, and seismic design parameters for hospital buildings are recommended.

## 5.2 CONCLUSIONS

The following are the important conclusions drawn from the study done as part of this thesis:

(1) Selection of appropriate structural system based on use and importance of building is very crucial to resist severe earthquakes—wall-frame structural system is recommended for hospital buildings situated in high seismic regions;
(2) Identification of suitable strain limit states to monitor structural damages at preferred seismic performance is crucial — *yielding* of longitudinal reinforcement in tension, *crushing* of extreme fibre of confined concrete in compression, and *spalling* of extreme fibre of unconfined concrete in compression, in select structural members are the strain limit states identified;
(3) Occurrence of limit state of the yielding of first layer of longitudinal reinforcement in tension first, in beams, columns or structural walls map well (but stringently) with *Occupiability* performance requirement in hospital buildings as it indicates a gradual transition from a state of no structural damage to structural damage, in typical *important*, low rise RC wall-frame hospital buildings. Thus, this limit state is regarded as the significant limit state for monitoring the beginning of structural damages.
(4) Provision of wall-frame structural systems with SPD of at least 3% is recommended for hospital buildings in high seismic regions and use of CBSR of at least 2 will

preclude damages in columns will ensure Occupiability seismic performance in hospital buildings; and

(5) Location and orientation of lateral load resisting elements should be appropriate to avoid undesirable modes of oscillation—static eccentricity about 5 m is observed to provide reasonably good linear and nonlinear behaviour.

## 5.3 LIMITATIONS OF PRESENT STUDY AND SCOPE FOR FUTURE WORK

The present study has the following limitations:

(a) Seismic behaviour is investigated of regular low rise RC wall-frames with fixed base, typical storey height and founded on soft soil. Variations in the above may alter the seismic behaviour of the buildings;
(b) Effect of unreinforced masonry walls are not considered in seismic of these buildings; and
(c) Only flexural damages are considered; shear hinges are not defined in structural members of these buildings;

Based on results of present study, following is the list of future work in this subject:

(a) A study may be undertaken by considering the effect of unreinforced masonry walls;
(b) A study may be undertaken by considering the influence of irregularities in plan, and elevation;
(c) A study may be undertaken by considering the influence of soil-structure interaction, especially if buildings are founded on soft soil; and
(d) A study may be undertaken by considering the effect of Nonstructural Elements, because of large number of these forming part of hospital buildings.

…

*Blank Page*

# References


[1] American Society of Civil Engineers (ASCE) (2022), *Minimum Design Loads for Buildings and Other Structure* (ASCE7-22), USA.

[2] American Society of Civil Engineer (ASCE) (2017), *Seismic Rehabilitation of Existing Buildings (ASCE/SEI 41-17),* USA.

[3] Anwar N., and Eng., D., (2009), "Modelling of Shear Walls for Non-linear and Pushover Analysis of Tall Buildings," *Proceedings of Fourteenth ASEP International Convection*, Thailand.

[4] Bertero, V.V., (1977), "Strength and Deformation Capacities of Buildings under Extreme Environments," *Structural Engineering and Structural Mechanics*, Pister KS (ed), Prentice Hall, Englewood Cliff, NJ, Vol. 53, pp.211-215.

[5] Bertero, V.V., (1980), "Seismic Behaviour of R/C Wall Structural Systems," *Proceedings of the Seventh World Conference on Earthquake Engineering*, Istanbul, Turkey, Vol.6, Article 323.

[6] Bureau of Indian Standards (BIS) (2016), *Criteria for Earthquake Resistant Design of Structure-Part 1 General Provisions and Buildings* (IS1893 (Part1): 2016), New Delhi, India.

[7] Bureau of Indian Standards (BIS), (2016), *Ductile Detailing of Reinforced Concrete Structure Subjected to Seismic Forces- Code of Practice* (IS 13920: 2016), New Delhi, India.

[8] Bureau of Indian Standards (BIS), (2000), *Plain and Reinforced Concrete – Code of Practice* (IS456:2000), New Delhi, India.

[9] Cred, C., (2020), "Human Cost of Disasters (2000-2019)," *United Nations Office of the Disarmament Affairs*, No. 61.

[10] Chen, H., Quancai, X., Feng, B., Liu, J., Huang, Y., and Chen Hongfu, (2017), "Seismic Performance to Emergency Centers, Communication and Hospital Facilities Subjected to Nepal Earthquake, 2015," Journal of Earthquake Engineering, Taylor & Francis Group. DOI: 10.1080/13632469.2017.1286623.

[11] Chung, R., Ballantyne, D., Corneau, E., and Holzer, T., (1996), US Department of Commerce, Technology Administration, *National Institute of Standards and Technology*, NIST Special Publication 901.

[12] CSI (2018), *Nonlinear Analysis and Performance Assessment for 3D Structures*, PERFORM-3D, Computers and Structures Inc., Berkeley, U.S.A.

[13] Deshmukh, A.B., (2017), *Optimal Use of RC Walls in Improving Earthquake Behaviour of RC Moment Frame Buildings on Hill Slopes*, MS Thesis, Indian Institute of Technology Madras, Chennai, India.

[14] DesRoches R., Comerio, M., Eberhard, M., Mooney, M., and Rix, J, G., (2011), "Overview of the 2010 Haiti Earthquake," *Earthquake Spectra*, EERI, Volume 27, No. S1, pp. S1-S21.

[15] EERI (1998), Annotated Slide Collection CD-ROM, Earthquake Engineering Research Institute, Oakland, CA.

[16] Elnashai, A.S., and Di Sarno, L., (2008), *Fundamentals of Earthquake Engineering*, John Wiley and Sons, United Kingdom.

[17] El-Tawil, S., Harries, K.A., Fortney, B.M., and Shahrooz, Y.K., (2010), "Seismic Design of Hybrid Coupled Wall Systems: State of the Art," *Journal of Structural Engineering*, ASCE, Vol.7, Issue 7, pp. 755-769.

[18] Eshghi, S., and Naserasadi, K., (2005), "Performance of Essential Buildings in 2003 Bam," *Earthquake Spectra*, EERI, Vol. 21, No. S1, pp. S375-S393.

[19] Fahjan, Y., Doran, B., Akbs B., and Kubin, J., (2012), "Pushover Analysis for Performance-based Seismic Design of RC Frames with Shear Walls," *Proceedings of the Fifteen World Conference on Earthquake Engineering*, Lisboa, Portugal, paper No.-4059.

[20] Fahjan, Y., Kubin, J., and Tan, M.T., (2010), "Nonlinear Analysis Methods for Reinforced Concrete Buildings with Shear Walls," *Proceedings of the Fourteen European Conference on Earthquake Engineering*, Ohrid, Republic of Macedonia, Volume 5.

[21] Federal Emergency Management Agency (FEMA), (2000), *Prestandard and Commentary for the Seismic Rehabilitation of Buildings*, FEMA 356, Washington DC.

[22] Fintel, M., and Ghosh, S. K., (1977) "Structural Systems for Earthquake -Resistant Concrete Buildings," *Proceedings of the Workshop on Earthquake Resistant Design of Reinforced Concrete Building Construction*, University of California, Berkeley, pp. 707-741.

[23] Fintel, M., (1995), "Performance of Buildings with Shear Walls in Earthquakes of Last Thirty Years", *PCI Journal, Precast/Prestressed Concrete Institute*, Chicago, Vol.40, No.3, pp.62-80.

[24] Hancock, J., Watson-Lamprey, J., Abrahamson, N.A., Bommer, J.J., Markatis, A., McCoyh, E., and Mendis, R., (2006)," An Improved Method of Matching Response of Recorded Earthquake Ground Motion using Wavelets," *Journal of Earthquake Engineering, Taylor and Francis*, Vol10, Special Issue 1, pp.67-89.

[25] Haselton, C.B., Whittaker A.S., Hortacsu, A., Baker, J.W., Bray, J., and Grant, D.N., (2012), "Selecting and Scaling Earthquake Ground Motions for Performing Response-History Analyses," *Proceedings of the Fifteen World Conference on Earthquake Engineering*, Lisboa, Portugal, paper no.-5552.

[26] Housner, G.W., and Jennings, P.C., (1982), *Earthquake Design Criteria*, EERI Monograph Series, Earthquake Engineering Research Institute, Oakland, California, USA.

[27] Huang, Y.-N., Whittaker, A.S., Luco, N., and Hamburger, R.O., (2011), "Scaling Earthquake Ground Motions for Performance-Based Assessment of Buildings," *Journal of Structural Engineering*, ASCE, Vol. 137, No.3, pp. 311-321.

[28] Inel, M. and Ozmen, Hayri., (2006), "Effects of Plastic Hinge Properties in Nonlinear Analysis of Reinforced Concrete Buildings", *Engineering Structures*, Elsevier, Vol.28, Issue 11, pp.1494-1502.

[29] Kalkan, E., and Chopra, A., (2010), "*Practical Guidelines to Select and Scale Earthquake Records for Nonlinear Response History Analysis of Structures*," Open-File Report, EERI and USGS, USA.

[30] Kent, D.C., and Park, R., (1971), "Flexural Members with Confined Concrete," *Journal of Structural Division*, ASCE, Vol.97, ST7, pp.1969-1990.

[31] Krishnamurthi, C., (2018), "Hospital Preparedness and Response During Earthquakes," *IOSR Journal of Dental and Medical Science-JDMS*, IOSR, Vol. 17, No.1, pp 53-57

[32] Kurama, Y. C., and Farrow, K. T., (2003), "Ground Motion Scaling Methods for Different Site Conditions and Structure Characteristics," *Earthquake Engineering and Structural Dynamics*, Vol. 32, Issue 15, pp.2425-2450.

[33] Jain S K and Navin R, "Seismic Overstrength in Reinforced Concrete Frames," *Journal of Structural Engineering*, ASCE, Vol. 121, No. 3, March 1995, pp 580-585.

[34] Jiang, H., and Liu, L., (2011), "Numerical Analysis of RC Shear Walls under Cyclic Loading by PERFORM 3D," *Advanced Materials Research*, Trans Tech Publications, Switzerland, Vol. 250-253, pp. 2253-2257.

[35] Lagos, R., Kupfer, M., Lindenberg, J., Bonelli, P., Saragoni, R., Guendelman, T., Massone, L, Boroschek, R., and Yanez, F., (2017) "Seismic Performance of Concrete Buildings in Chile," *Proceedings of the Sixteenth World Conference on Earthquake Engineering, Santiago*, Chile, paper no. 3769.

[36] Lew, H.S., Leyendecker, E.V., and Dikkers, R.D, (1975), "*Engineering Aspects of the 1971 San Fernando Earthquake,*" US Department of Commerce, National Bureau of Standards, Building Science Series 40.

[37] Lu, Y., (2001), "Seismic behaviour of multistory RC wall-frame systems versus bare ductile frame system," *Earthquake Engineering and Structural Dynamics*, Vol. 31, No.(1), pp. 79–97 (2001).

[38] Mander, J.B., Priestly, M.J.N., and Park, R., (1988), "Theoretical Stress- Strain Model for Confined Concrete," *Journal of Structural Engineering*, ASCE, Vol.114, No.8, pp.1804-1826.

[39] Mattock, A.H., (1967), "Discussion of Rotational Capacity of Hinging Regions in Reinforced Concrete Beams," by W.G. Corley, *Journal of Structural Division*, ASCE, Vol.93, ST2, pp.519-522.

[40] Mittal, H., Kumar, A., and Ramhmachhuani, R., (2012), "Indian national strong motion instrumentation network and site characterization of its stations," *Int J Geosci*, Vol. 3, No. 6A, pp. 1151-1167.

[41] Mitchell, D., DeVall, R.H., Saatcioglu, M., Simpson, R., Tinnawi, R., and Tremblay, R., (1995), "Damage to Concrete Structures due to the 1994 Northridge Earthquake," *Canadian Journal of Civil Engineering*, Vol.22, No. 2, pp.361-371.

[42] Murty, C.V.R., Goswami, R., Vijaynarayanan, A.R., Mehta, V.V., (2012), "*Some Concepts on Earthquake Behaviour of Buildings*", Gujarat State Disaster Management Authority, Gandhinagar.

[43] Naeim, F., Lew, M., Carpenter, L.D., Youssef, N.F., Rojas, F., Saragoni, G.R., and Adaros, M.S., (2010), "Performance of Tall Buildings in Santiago, Chile During the 27

February 2010 Offshore Maule, Chile Earthquake." *The Structural Design of Tall and Special Buildings*, Vol.20, No.1, pp. 1-16.

[44] Nassar, A.A., and Krawinkler, H., (1991), *Seismic Demands on SDOF and MDOF Systems*, The John A. Blume Earthquake Engineering Center, Report N0.95, Stanford University, Stanford, USA.

[45] National Disaster Management Authority Government of India, (2016), *National Disaster Management Guidelines Hospital Safety*, New Delhi, India.

[46] Newmark, N.M., and Hall. W.J. (1973), "*Procedures and Criteria for Earthquake Resistant Design*," Building Practices for Disaster Mitigation, Proceedings, edited by Wright R., Kramer, S., and Culver, C., Building Science Series No.46, National Bureau of Standards, and U.S. Department of Commerce, Washington, D.C., Appendix B, pp.209-236.

[47] Otani, S., (1977), "Earthquake Tests of Shear Wall-Frame Structures to Failure," *Proceedings of the Sixth World Conference on Earthquake Engineering*, New Delhi, Vol. 3, pp. 2759-2765.

[48] Ozkul, A. T., Kurtbeyoglu, A., Borekci, M., Zengin, B., and Kocak, A., (2019), "Effect of Shear Wall on Seismic Performance of RC Frame Buildings," *Engineering Failure Analysis*, Elsevier, Vol. 100, pp.60–75.

[49] Orakcal, K., Wallace, J.W., and Conte, J.P., (2004), "Flexural Modeling of Reinforced Concrete Walls-model Attributes," *Structural Journal*, ACI, Vol. 101, No. 5, pp.688–698.

[50] Panagiotou, M., Restrepo, J., Schoettler, M., and Kim, G., (2012), "Nonlinear Cyclic Truss Model for Reinforced Concrete Walls," *Structural Journal*, ACI, Vol.109 (2), pp.205–214.

[51] Park, R., and Paulay, T., (1975b), *Reinforced Concrete Structures*, John Wiley & Sons, UK.

[52] Paulay, T., and Priestley, M.J.N., (1992), *Seismic Design of Reinforced Concrete and Masonry Buildings, John Wiley and Sons*, New York, ISBN:978-0-471-54915-4.

[53] Rai, D.C., Jain, S.K., and Chakrabarti, I., (2012), "Evaluation of Properties of Steel Reinforcing Bars for Seismic Design," *Proceedings of the Fifteen World Conference on Earthquake Engineering*, Lisboa, Portugal, paper no. 3720.

[54] Rana, R., Limin, J., and Atila Z., (2004) "Pushover Analysis of a 19 Story Concrete Shear Wall Building," *Proceedings of the Thirteenth World Conference on Earthquake Engineering*, Vancouver, B.C., Canada, paper no. 133.

[55] Razvi, S.R., and Saatcioglu, M., (1994), "Strength and Deformability of Confined High-Strength Concrete Columns," *Structural Journal*, ACI, Vol.91, No.6, pp678-687.

[56] Reitherman, R., (2006), "Earthquakes that have Initiated the Development of Earthquake Engineering," *Bulletin of the New Zealand Society for Earthquake Engineering*, Vol.39, No.3, pp.145-157.

[57] Riddell, R., Hidalgo, P., and Cruz, E., (1989), "Response Modification Factors for Earthquake Resistant Design of Short Period Buildings," *Earthquake Spectra*, Vol. 5, Issue 3, pp. 571-590.

[58] Roy, N., Shah, H., Patel, V., and Richard Coughlin, R., (2003), "The Gujarat Earthquake (2001) Experience in a Seismically Unprepared Area: Community

Hospital Medical Response," *Prehospital and Disaster Medicine*, Vol. 17, No.4, pp.186-195.

[59] Saatcioglu, M., and Razvi, S., (1992)," Strength and Ductility of Confined Concrete," *Journal of Structural Engineering*, ASCE, Vol. 118, Issue 6, pp. 1590-1607.

[60] Sawyer, H.A., (1964), "Design of Concrete Frames for Two Failure States," *Proceedings of the International Symposium on the Flexural Mechanics of Reinforced Concrete*, ASCE-ACI, pp.405-431.

[61] Stone, W.C., and Felix, Y.Y., (1987), "Engineering Aspects of September 19, 1985 Mexico Earthquakes," US Department of Commerce, National Bureau of Standards, NBS Building Science Series, 165.

[62] Sunitha, P., (2017), "*Seismic Design of Low-rise RC Moment Frame Buildings Rationalised with Earthquake Resistant Design Philosophy*," Ph.D. Thesis, Indian Institute of Technology Madras, Chennai, India.

[63] Sunitha, P., Goswami, R., and Murty, C.V.R., (2021), "Design of RC moment frame buildings consistent with earthquake resistant design philosophy," *Earthquakes and Structures*, Vol. 20, No. 6, pp.599-615.

[64] Todd, D., Carino N., Chung R.M., Lew, H.S., Taylor, A.W., Walton, W.D., Copper, K.D., and Nimis, R., (1994), "1994 Northridge Earthquake Performance of Structures, Lifelines and Fire Protection Systems," US Department of Commerce, Technology Administration, *National Institute of Standards and Technology*, NIST Special Publications 862.

[65] Ugalde, D., and Lopez-Garcia, D., (2017), "Behaviour of Reinforced Concrete Shear Wall Buildings Subjected to Large Earthquake," *Procedia Engineering*, Vol. 199, pp.3582-3587.

[66] Vamvatsikos, D., and Cornell, C.A., (2002), "Incremental Dynamic Analysis," *Earthquake Engineering and Structural Dynamics*, Vol.31, No.3, pp.491-514.

[67] Vijayanarayanan, A.R., Goswami, R., and Murty, C.V.R., (2022), "A Method for Seismic Design of RC Frame Buildings using Fundamental Mode and Plastic Rotation Capacity," *Bulletin of the New Zealand Society for Earthquake Engine*ering, Vol. 55, No.2, pp.112-128.

[68] Yeong, A.H., Kunnath, S.K., and Abrahamson, N., (2011), "Amplitude Matched versus Spectrum-Matched Ground Motions for Seismic Performance Assessment," *Journal of Structural Engineering*, ASCE, Vol. 137, No. 3, pp.278-288.

...

# Annexure A

## Design Details of Study Buildings

### A.0 OVERVIEW

Numerical work in the present study comprises of two sections, namely (a) pilot study conducted on 2D Wall-Frames varying the plan aspect ratio (presented in Chapter 3), and (b) study on 3D hospital building (presented in Chapter 4). In the second part of the study on 3D buildings, Buildings A, B and C are moment frames and Buildings D, E, F and G wall-frames with structural configurations of varying SPD of structural walls. Cross-section details of structural members are provided in Table A.1, Tables A.2 and Table A.3. Seven 3D building (Figures A.1-A.3) details are presented in Table A.1 and A.2. Six 2D wall-frames has thickness 250 mm, and the length corresponding to wall plan aspect ratios of 4, 8, 12, 16, 20 and 24 (Table A.3).

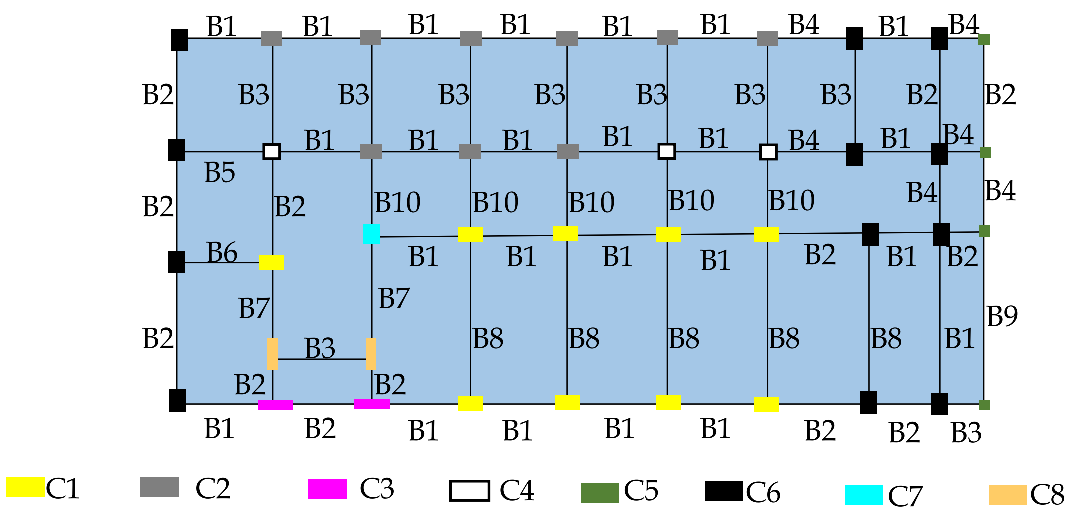


**Figure A.1**: Structural plan of Building A

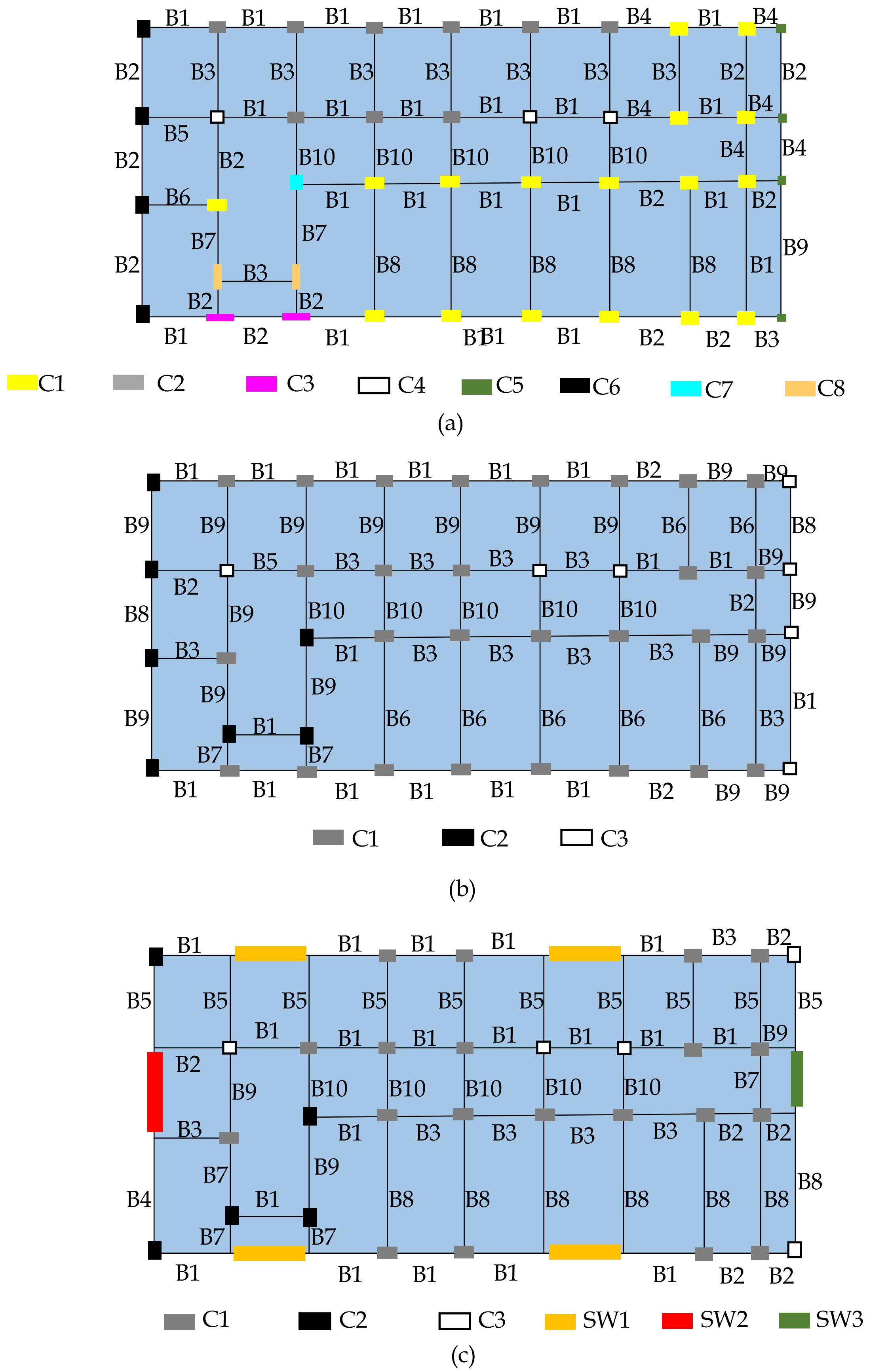


**Figure A.2**: Structural plan of buildings: (a) B, (b) C, and (c) D

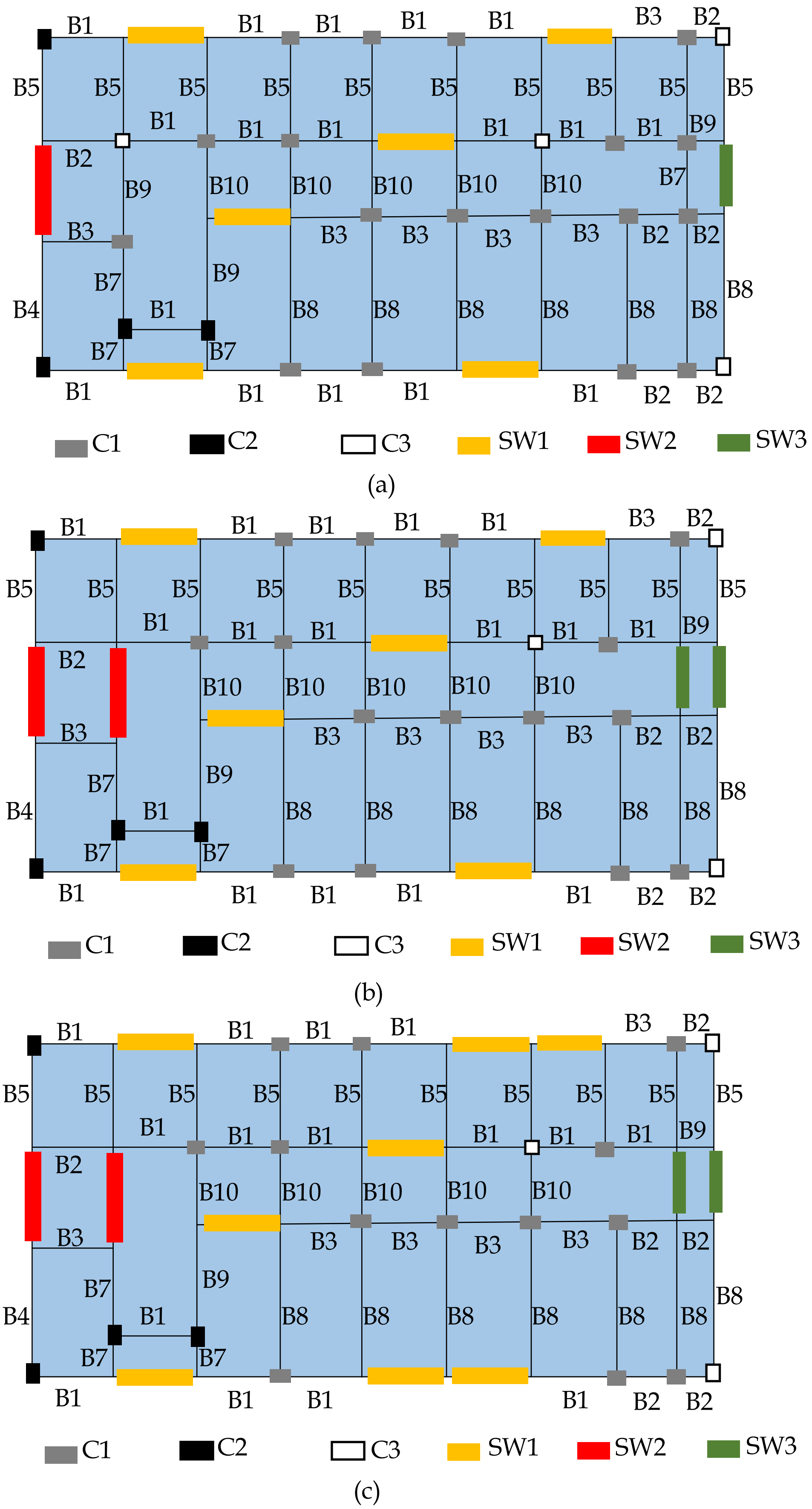


**Figure A.3**: Structural plan of buildings: (a) E, (b) F, and (c) G

**Table A.1**: Reinforcement details of beams and columns of hospital building

| Building | Member | Beam | | | | | | | | | | Column | | | | | | | |
|---|---|---|---|---|---|---|---|---|---|---|---|---|---|---|---|---|---|---|---|
| | Type | B1 | B2 | B3 | B4 | B5 | B6 | B7 | B8 | B9 | B10 | C1 | C2 | C3 | C4 | C5 | C6 | C7 | C8 |
| A/B | Width (mm) | 250 | | | | | | | | | | 750 | 750 | 1000 | 500 | 350 | 350 | 300 | 250 |
| | Depth (mm) | 550 | | | | | | | | | 500 | 350 | 300 | 250 | 500 | 350 | 750 | 750 | 1000 |
| | Longitudinal reinforcement(%) | 1.88, 1.36 | 1.53, 0.94 | 1.39, 0.94 | 1.88, 1.36 | 0.45, 1.36 | 0.29, 1.06 | 0.91, 0.68 | 2.14, 1.36 | 0.74, 0.60 | 1.25, 1.25 | 2.5 | 2.54 | 2.35 | 1.64 | 3.2 | 2.5 | 2.54 | 2.35 |
| | Transverse Rebar | Y8@150 | | | | | | | | | Y8@90 | Y10@100 | | Y8@75 | Y10@100 | | | | |
| | Type | B1 | B2 | B3 | B4 | B5 | B6 | B7 | B8 | B9 | B10 | C1 | | | C2 | | | C3 | |
| | Width (mm) | 250 | | | | | | | | | | 750 | | | 500 | | | 500 | |
| | Depth (mm) | 550 | | | | | | | | | 500 | 500 | | | 750 | | | 500 | |
| C | Longitudinal reinforcement(%) | 1.00, 0.60 | 1.12, 0.60 | 1.07, 0.54 | 0.87, 0.45 | 1.12, 0.60 | 1.42, 0.71 | 0.80, 0.46 | 0.86, 0.43 | 0.94, 0.51 | 0.84, 0.48 | 1.2 | | | 2.2 | | | 1.2 | |
| | Transverse Rebar | Y10@100 | | | | | | | | | | Y10@100 | | | | | | | |
| D | Longitudinal reinforcement(%) | 0.91, 0.45 | 0.71, 0.37 | 0.68, 0.37 | 0.79, 0.43 | 0.77, 0.43 | 0.68, 0.37 | 0.53, 0.29 | 0.94, 0.52 | 0.68, 0.35 | 0.75, 0.45 | 1.0 | | | 1.5 | | | 1.0 | |
| | Transverse Rebar | Y10@100 | | | | | | | | | | Y10@100 | | | | | | | |
| E | Longitudinal reinforcement(%) | 0.85, 0.46 | 0.45, 0.29 | 0.60, 0.34 | 0.71, 0.37 | 0.70, 0.35 | 0.50, 0.29 | 0.50, 0.29 | 0.85, 0.46 | 0.60, 0.35 | 0.57, 0.32 | 1.0 | | | 1.5 | | | 1.0 | |
| | Transverse Rebar | Y10@100 | | | | | | | | | | Y10@100 | | | | | | | |
| F | Longitudinal reinforcement(%) | 0.80, 0.43 | 0.42, 0.29 | 0.57, 0.32 | 0.70, 0.35 | 0.70, 0.35 | 0.42, 0.29 | 0.42, 0.29 | 0.80, 0.43 | 0.55, 0.29 | 0.56, 0.29 | 1.0 | | | 1.5 | | | 1.0 | |
| | Transverse Rebar | Y10@100 | | | | | | | | | | Y10@100 | | | | | | | |
| G | Longitudinal reinforcement(%) | 0.78, 0.40 | 0.42, 0.29 | 0.55, 0.32 | 0.63, 0.35 | 0.60, 0.32 | 0.42, 0.29 | 0.58, 0.29 | 0.78, 0.40 | 0.51, 0.29 | 0.56, 0.29 | 1.0 | | | 1.5 | | | 1.0 | |
| | Transverse Rebar | Y10@100 | | | | | | | | | | Y10@100 | | | | | | | |

**Table A.2**: Reinforcement details of structural wall of hospital building

| Building | Member | Wall Web | | | | | Wall Boundary Element | |
|---|---|---|---|---|---|---|---|---|
| | | Dimensions ($d_w \times t_w$) | Vertical reinforcement | | Horizontal reinforcement | | Longitudinal reinforcement (%) | Dimensions ($b_f \times t_f$) |
| | | | Diameter | Spacing (mm) | Diameter | Spacing (mm) | | |
| D | SW 1 | 6500 x 250 | Y 10 | 210 | Y 8 | 160 | Not required | Not required |
| | SW 2 | 3200 x 250 | Y 10 | 200 | Y 10 | 180 | 1.57 | 500 x 250 |
| | SW 3 | 2000 x 250 | Y 10 | 180 | Y 10 | 200 | 2.35 | 500 x 250 |
| E | SW 1 | 6500 x 350 | Y 10 | 200 | Y 8 | 160 | Not required | Not required |
| | SW 2 | 3200 x 350 | Y 10 | 190 | Y 10 | 160 | 1.21 | 500 x 350 |
| | SW 3 | 2000 x 350 | Y 10 | 150 | Y 10 | 200 | 1.68 | 500 x 350 |
| F | SW 1 | 6500 x 450 | Y 10 | 140 | Y 8 | 110 | Not required | Not required |
| | SW 2 | 3200 x 450 | Y 10 | 110 | Y 10 | 110 | 0.9 | 500 x 450 |
| | SW 3 | 2000 x 450 | Y 10 | 100 | Y 10 | 110 | 1.30 | 500 x 450 |
| G | SW 1 | 6500 x 500 | Y 10 | 120 | Y 8 | 100 | Not required | Not required |
| | SW 2 | 3200 x 500 | Y 10 | 100 | Y 10 | 100 | 0.8 | 500 x 500 |
| | SW 3 | 2000 x 500 | Y 10 | 100 | Y 10 | 100 | 1.17 | 500 x 500 |

*Note*: “Not required” indicates the non-requirement of boundary element as per IS13920 (2016)



**Table A.3**: Cross-section details of 2D wall-frames considered for pilot study

| | *Structural wall* | *Aspect Ratio* | | 4 | 8 | 12 | 16 | 20 | 24 |
|---|---|---|---|---|---|---|---|---|---|
| *Reinforcement* | *Beam* | *Longitudinal (%)* | | 1.30 | 1.11 | 0.92 | 0.78 | 0.72 | 0.64 |
| | | | | 0.65 | 0.55 | 0.46 | 0.39 | 0.36 | 0.32 |
| | *Column* | *Longitudinal:* 2%<br>*Transverse*: Y10 @ 100 mm c/c | | | | | | | |
| | *Wall Web* | *Vertical* | Y10 | | | | | | |
| | | | Spacing (mm) | 110 | 150 | 170 | 190 | 200 | 210 |
| | | *Horizontal* | Y10 | | | | | | |
| | | | Spacing (mm) | 220 | 250 | | | | |
| | *Wall Boundary Element* | *Longitudinal (%)* | | 3.6 | 3.6 | 3.0 | 2.0 | 0.72 | 0.72 |
| | | *Transverse*: | Y10@100 mm c/c | | | | | | |